

¹ Increasing prevalence of plant-fungal symbiosis across two
² centuries of environmental change

³ Joshua C. Fowler^{1,2*}

Jacob Moutouama^{1,3}

Tom E. X. Miller¹

⁴ 1. Rice University, Department of BioSciences, Houston, Texas 77006; 2. University of Miami,
⁵ Department of Biology, Miami, Florida; 3. Department of Botany, University of British Columbia,
⁶ 6270 University Blvd, Vancouver, BC V6T 1Z4

⁷ * Corresponding author; e-mail: jcf221@miami.edu.

⁸ *Manuscript elements:* Figure 1 - Figure 6, Appendix A (including Figure A1 - Figure A15, Table
⁹ A1, and Supporting Methods).

¹⁰ *Keywords:* climate change, *Epichloë*, herbarium, INLA, museum specimen, plant-microbe sym-
¹¹ biosis, *Poaceae*, spatially-varying coefficients model

¹² *Manuscript type:* Research Article.

Abstract

Species' distributions and abundances are shifting in response to ongoing global climate change. Mutualistic microbial symbionts can provide hosts with protection from environmental stress that may promote resilience under environmental change, however this change may also disrupt species interactions and lead to declines in hosts and/or symbionts. Symbionts preserved within natural history specimens offer a unique opportunity to quantify changes in microbial symbiosis across broad temporal and spatial scales. We asked how the prevalence of seed-transmitted fungal symbionts of grasses (*Epichloë* endophytes) has changed over time in response to climate change, and how these changes vary across host species' distributions. Specifically, we examined 2,346 herbarium specimens of three grass host species (*Agrostis hyemalis*, *Agrostis perennans*, *Elymus virginicus*) collected over the past two centuries (1824 – 2019) for the presence or absence of *Epichloë* symbiosis. Analysis of an approximate Bayesian spatially-varying coefficients model revealed that endophytes increased in prevalence over the last two centuries from ca. 25% to ca. 75% prevalence, on average, across three host species. Changes in seasonal climate drivers were associated with increasing endophyte prevalence. Notably, increasing precipitation during the peak growing season for *Agrostis* species and decreasing precipitation for *E. virginicus* were associated with increasing endophyte prevalence. Changes in the variability of precipitation and temperature during off-peak seasons were also important predictors of increasing endophyte prevalence. Our analysis performed favorably in an out-of-sample predictive test with contemporary survey data from across 63 populations, a rare extra step in collections-based research. We identified greater local-scale variability in endophyte prevalence in contemporary data compared to model predictions based on historic data, suggesting new directions that could improve predictive accuracy. Our results provide novel evidence for a cryptic biological response to climate change that may contribute to the resilience of host-microbe symbiosis through fitness benefits to symbiotic hosts.

Introduction

38 Understanding how biotic interactions are altered by global change is a major goal of basic and
39 applied ecological research (Blois et al., 2013; Gilman et al., 2010). Documented responses to envi-
40 ronmental change, such as shifts in species' distributions (Aitken et al., 2008) and phenology (Piao
41 et al., 2019), are typically blind to concurrent changes in associated biotic interactions. Empirically
42 evaluating these biotic changes – whether interacting species shift in tandem with their partners
43 or not (HilleRisLambers et al., 2013) – is crucial to predicting the reorganization of Earth's biodi-
44 versity under global change. Such evaluations have been limited because few datasets on species
45 interactions extend over sufficiently long time scales of contemporary climate change (Poisot et al.,
46 2021).

47 Natural history specimens, which were originally collected to study and preserve taxonomic
48 diversity, present a unique opportunity to explore long-term changes in **biodiversity** and ecological
49 interactions across broad spatial and temporal scales (Davis, 2023; Meineke et al., 2018). Natural
50 history collections, built and maintained by the efforts of thousands of scientists, are invaluable
51 time machines, primarily comprised of physical specimens of organisms along with information
52 about the time and place of their collection. These specimens often preserve physical legacies of
53 ecological processes and species' interactions from dynamically changing environments across time
54 and space (Lendemer et al., 2020). For example, previous researchers have examined the flowers,
55 pollen grains, and leaves of specimens within plant collections (herbaria) collected across time to
56 document shifts in reproductive phenology (Berg et al., 2019; Park et al., 2019; Willis et al., 2017),
57 pollination (Duan et al., 2019; Pauw and Hawkins, 2011), and herbivory (Meineke et al., 2019)
58 related to anthropogenic climate change. However, few previous studies have leveraged biological
59 collections to examine climate change-related shifts in a particularly common type of interaction:
60 microbial symbiosis.

61 Microbial symbionts are common to all macroscopic organisms and can have important effects
62 on their hosts' survival, growth and reproduction (McFall-Ngai et al., 2013; Rodriguez et al., 2009).

63 Many microbial symbionts act as mutualists, engaging in reciprocally beneficial interactions with
64 their hosts that can ameliorate environmental stress. For example, bacterial symbionts of insects,
65 such as *Wolbachia*, can improve their hosts' thermal tolerance (Reno et al., 2019; Truitt et al., 2019),
66 and arbuscular mycorrhizal fungi, documented in 70-90% of families of land plants (Parniske, 2008),
67 allow their hosts to persist through drought conditions by improving water and nutrient uptake
68 (Cheng et al., 2021). On the other hand, changes in the mean and variance of environmental
69 conditions may disrupt microbial mutualisms by changing the costs and benefits of the interaction
70 for each partner in ways that can cause the interaction to deteriorate (Aslan et al., 2013; Fowler et al.,
71 2024). Coral bleaching (the loss of symbiotic algae) due to temperature stress (Sully et al., 2019)
72 is perhaps the best known example, but this phenomenon is not unique to corals. Lichens exposed
73 to elevated temperatures experienced loss of photosynthetic function along with changes in the
74 composition of their algal symbiont community (Meyer et al., 2022). How commonly and under what
75 conditions microbial mutualisms deteriorate or strengthen under climate change remain unanswered
76 questions (Frederickson, 2017). Previous work suggests that these alternative responses may depend
77 on the intimacy and specialization of the interaction as well as the physiological tolerances of the
78 mutualist partners (Rafferty et al., 2015; Toby Kiers et al., 2010; Warren and Bradford, 2014).

79 Understanding of how microbial symbioses are affected by climate change is additionally com-
80 plicated by spatial heterogeneity in the direction and magnitude of environmental change (IPCC,
81 2021). Beneficial symbionts are likely able to shield their hosts from environmental stress in loca-
82 tions that experience a small degree of change, but symbionts in locations that experience changes
83 of large magnitude may be pushed beyond their physiological limits (Webster et al., 2008). Ad-
84 ditionally, symbionts are often unevenly distributed across their host's distribution. Facultative
85 symbionts may be absent from portions of the host range (Afkhami et al., 2014), and hosts may en-
86 gage with a diversity of partners (different symbiont species or locally-adapted strains) across their
87 environments (Fowler et al., 2023; Frade et al., 2008; Rolshausen et al., 2018). Identifying broader
88 spatial trends in symbiont prevalence is therefore an important step in developing predictions for
89 where to expect changes in the symbiosis in future climates.

90 *Epichloë* fungal endophytes are specialized symbionts of cool-season grasses, which have been
91 documented in ~ 30% of cool-season grass species (Leuchtmann, 1992). They are predominantly
92 transmitted vertically from maternal plants to offspring through seeds. Vertical transmission cre-
93 ates a feedback between the fitness of host and symbiont (Douglas, 1998; Fine, 1975; Rudgers et al.,
94 2009). Over time, endophytes that act as mutualists should rise in prevalence within a host pop-
95 ulation, particularly under environmental conditions that elicit protective benefits (Donald et al.,
96 2021). *Epichloë* are known to improve their hosts' drought tolerance (Decunta et al., 2021) and
97 protect their hosts against herbivores (Crawford et al., 2010) and pathogens (Xia et al., 2018) likely
98 through the production of a diverse suite of alkaloids and other secondary metabolites. The fitness
99 feedback induced by vertical transmission leads to the prediction that endophyte prevalence should
100 be high in populations where these fitness benefits are most important. Previous survey studies
101 of contemporary populations have documented large-scale spatial patterns in endophyte prevalence
102 structured by environmental gradients (Afkhami, 2012; Bazely et al., 2007; Granath et al., 2007;
103 Sneck et al., 2017). We predicted that prevalence should track temporal changes in environmental
104 drivers (i.e. drought) that elicit strong fitness benefits.

105 Early research on *Epichloë* used herbarium specimens to describe the broad taxonomic diversity
106 of host species that harbor these symbionts (White and Cole, 1985), establishing that endophyte
107 symbiosis could be identified in plant tissue from as early as 1851. However, no subsequent studies,
108 to our knowledge, have used the vast resources of biological collections to quantitatively assess
109 spatio-temporal trends in endophyte prevalence and their environmental correlates. Previous work
110 has used herbarium specimens to identify the origins and population genomics of plant diseases such
111 as *Phytophthora*, the Irish potato famine pathogen (Ristaino et al., 2001; Ristaino, 2002; Yoshida et al.,
112 2013), and have been proposed as vehicles to track other emerging plant pathogens (Bradshaw et al.,
113 2021; Ristaino, 2020). Grasses are commonly collected and identified based on the presence of their
114 reproductive structures, meaning that preserved specimens typically contain seeds, conveniently
115 preserving the fungi along with their host plants on herbarium sheets. This creates the opportunity
116 to leverage the unique spatio-temporal sampling of herbarium collections to examine the response

117 of this symbiosis to historical climate change. However, the predictive ability derived from historical
118 analyses is rarely tested against contemporary data (Lee et al., 2024). Critically evaluating whether
119 insights from historical reconstruction are predictive of variation across contemporary populations
120 is a crucial step for the field to move from reading signatures of the past to forecasting ecological
121 dynamics into the future.

122 In this study, we assessed the long-term responses of *Epichloë* endophyte symbiosis to climate
123 change through the use of herbarium specimens of three North American host grass species (*Agrostis*
124 *hyemalis*, *Agrostis perennans*, and *Elymus virginicus*). We first addressed questions describing
125 spatial and temporal trends in endophyte prevalence: (i) How has endophyte prevalence changed
126 over the past two centuries? and (ii) How spatially variable are temporal trends in endophyte
127 prevalence across eastern North America? We then addressed how climate change may be driving
128 trends in endophyte prevalence by asking: (iii) What is the relationship between temporal trends
129 in endophyte prevalence and associated changes in climate drivers? We predicted that overall
130 endophyte prevalence would increase over time in tandem with climate change, and that localized
131 hotspots of endophyte change would correspond spatially to hotspots of climate warming and drying.
132 Finally, we evaluated (iv) how our model, built on data from historic specimens, performed in an out-
133 of-sample test using data on endophyte prevalence from contemporary surveys of host populations.
134 To answer these questions we examined a total of 2,346 historic specimens collected across eastern
135 North America between 1824 and 2019, and evaluated model performance against contemporary
136 surveys comprising 1,442 individuals from 63 populations surveyed between 2013 and 2020.

137 Methods

138 *Focal species*

139 Our surveys focused on three native North American grasses: *Agrostis hyemalis*, *Agrostis perennans*,
140 and *Elymus virginicus* that host *Epichloë* symbionts. These cool-season grass species are commonly
141 represented in natural history collections with broad distributions covering much the eastern United

¹⁴² States (Fig. 1). Cool-season grasses grow during the cooler temperatures of spring and autumn
¹⁴³ due to their reliance on C_3 photosynthesis. *A. hyemalis* is a small short-lived perennial species
¹⁴⁴ that germinates in late winter/early spring and typically flowers between March and July (most common
¹⁴⁵ collection month: May). *A. perennans* is of similar stature but is longer lived than *Agrostis hyemalis*
¹⁴⁶ and flowers in late summer and early autumn (most common collection month: September). *A.*
¹⁴⁷ *perennans* is more sparsely distributed, tending to be found in shadier and moister habitats, while
¹⁴⁸ *A. hyemalis* is commonly found in open and recently disturbed habitats. Both *Agrostis* species are
¹⁴⁹ recorded from throughout the Eastern US, but *A. perennans* has a slightly more northern distri-
¹⁵⁰ bution, whereas *A. hyemalis* is found rarely as far north as Canada and is listed as a rare plant
¹⁵¹ in Minnesota. *E. virginicus* is a larger and relatively longer-lived species that is more broadly dis-
¹⁵² tributed than the *Agrostis* species. It begins flowering as early as March or April but continues
¹⁵³ throughout the summer (most common collection month: July).

¹⁵⁴ Both *Agrostis* species host *Epichloë amarillans* (Craven et al., 2001; Leuchtmann et al., 2014),
¹⁵⁵ while *Elymus virginicus* typically hosts *Epichloë elymi* (Clay and Schardl, 2002). The fungal sym-
¹⁵⁶ bionts primarily reproduce asexually and are passed from mother to offspring by vertical transmis-
¹⁵⁷ sion through seeds. These traits contribute to highly specialized interactions between symbiont and
¹⁵⁸ host. Some host species have been shown to partner with multiple symbiont species or strains, and in
¹⁵⁹ some cases multiple symbiont lineages can co-exist within a host population (Mc Cargo et al., 2014).
¹⁶⁰ However, surveys have typically found limited *Epichloë* genotypic diversity within host populations
¹⁶¹ (Treindl et al., 2023). Across host populations, concentrations of biologically-active alkaloids and
¹⁶² the genes associated with their production vary substantially (Schardl et al., 2012). In this analysis,
¹⁶³ we focus on the presence/absence of *Epichloë* symbionts, and we discuss potential implications of
¹⁶⁴ symbiont genotypic diversity in the Discussion.

¹⁶⁵ *Herbarium surveys*

¹⁶⁶ We visited nine herbaria between 2019 and 2022 (see Table A1 for a summary of specimens included
¹⁶⁷ from each collection). With permission from herbarium staff, we acquired seed samples from 1135

¹⁶⁸ *A. hyemalis* specimens collected between 1824 and 2019, 357 *A. perennans* specimens collected
¹⁶⁹ between 1863 and 2017, and 854 *E. virginicus* specimens collected between 1839 and 2019 (Fig. 1,
¹⁷⁰ Fig. 2A, Fig. A1). We chose our focal species in part because they are commonly represented in
¹⁷¹ herbarium collections and produce many seeds, meaning that small samples would not diminish the
¹⁷² value of the specimens for future studies. We collected 5-10 seeds per specimen after examining the
¹⁷³ herbarium sheet under a dissecting microscope to ensure that we collected mature seeds, not florets
¹⁷⁴ or unfilled seeds, fit for our purpose of identifying fungal endophytes with microscopy. We excluded
¹⁷⁵ specimens for which information about the collection location and date were unavailable.

¹⁷⁶ Each specimen was assigned geographic coordinates based on collection information recorded on
¹⁷⁷ the herbarium sheet using the geocoding functionality of the ggmap R package (Kahle and Wickham,
¹⁷⁸ 2019). Many specimens had digitized collection information readily available, but for those that did
¹⁷⁹ not, we transcribed information printed on the herbarium sheet. Collections were geo-referenced
¹⁸⁰ to the nearest county centroid, or nearest municipality when that information was available. For
¹⁸¹ fifteen of the oldest specimens, only information at the state level was available, and so we used the
¹⁸² state centroid. The median pairwise distance between georeferenced coordinate points was 841 km.
¹⁸³ The median longitudinal width of the bounding boxes generated to geocode municipality, county, or
¹⁸⁴ state centroids was 44.7 km. Among those specimens geo-referenced at the state level, the largest
¹⁸⁵ bounding box, spanning the state of Texas, was 1233 km wide. The smallest bounding boxes were
¹⁸⁶ less than 1 km across for small municipalities (while this suggests high precision, we note that some
¹⁸⁷ specimens were collected in natural habitat nearby to small municipalities not encompassed by this
¹⁸⁸ bounding boxes).

¹⁸⁹ Our visits focused on herbaria with historic strengths in *Poaceae* collections (e.g. Texas A&M,
¹⁹⁰ Missouri Botanic Garden) and other herbaria in the Southern Great Plains region of the United
¹⁹¹ States. While these nine herbaria garnered specimens that span the focal species' ranges, our dataset
¹⁹² unevenly samples across the study region (Fig. 1). Texas, Oklahoma, Louisiana, and Missouri are
¹⁹³ the most represented states. Uneven sampling was most pronounced for *A. perennans*, which has
¹⁹⁴ much of its range in the northeastern US. We explore the potential influence of spatial bias in

195 sampling on our results through a simulation analysis (Appendix A - Supporting Methods).

196 After collecting seed samples, we quantified the presence or absence of *Epichloë* fungal hyphae
197 in each specimen using microscopy. We first softened seeds with a 10% NaOH solution, then stained
198 the seeds with aniline blue-lactic acid stain and squashed them under a microscope cover slip. We
199 examined the squashed seeds for the presence of fungal hyphae at 200-400X magnification (Bacon
200 and White, 2018). On average we scored 4.7 intact seeds per specimen of *A. hyemalis*, 4.2 seeds
201 per specimen of *A. perennans*, and 3.8 seeds per specimen of *E. virginicus*; we scored 10,342 seeds
202 in total. Due to imperfect vertical transmission, the production of symbiont-free offspring from
203 symbiotic hosts (Afkhami and Rudgers, 2008), it is possible that symbiotic host-plants produce a
204 mixture of symbiotic and non-symbiotic seeds. We therefore designated a specimen as endophyte-
205 symbiotic if *Epichloë* hyphae were observed in one or more of its seeds, or non-symbiotic if *Epichloë*
206 hyphae were observed in none of its seeds. To capture uncertainty in the endophyte identification
207 process, we recorded both a "liberal" and a "conservative" endophyte score for each plant specimen.
208 When we confidently identified endophytes within a specimen's seeds, we assigned matching liberal
209 and conservative scores. When we identified potential endophytes with unusual morphology, low
210 uptake of stain, or a small amount of fungal hyphae across the scored seeds, we recorded a positive
211 identification for the liberal score and a negative identification for the conservative score. 89% of
212 scored plants had matching liberal and conservative scores, reflecting high confidence in endophyte
213 status. The following analyses used the liberal status, however repeating all analyses with the
214 conservative status yielded qualitatively similar results (Fig. A8).

215 *Modeling spatial and temporal changes in endophyte prevalence*

216 We assessed spatial and temporal changes in endophyte prevalence across each host distribution,
217 quantifying the "global" temporal trends averaged across space, and then examining spatial hetero-
218 geneity in the direction and magnitude of endophyte change (hotspots and coldspots) across the spa-
219 tial extent of each host's distribution. To account for the spatial non-independence of geo-referenced
220 occurrences, we used an approximate Bayesian method, Integrated Nested Laplace Approximation

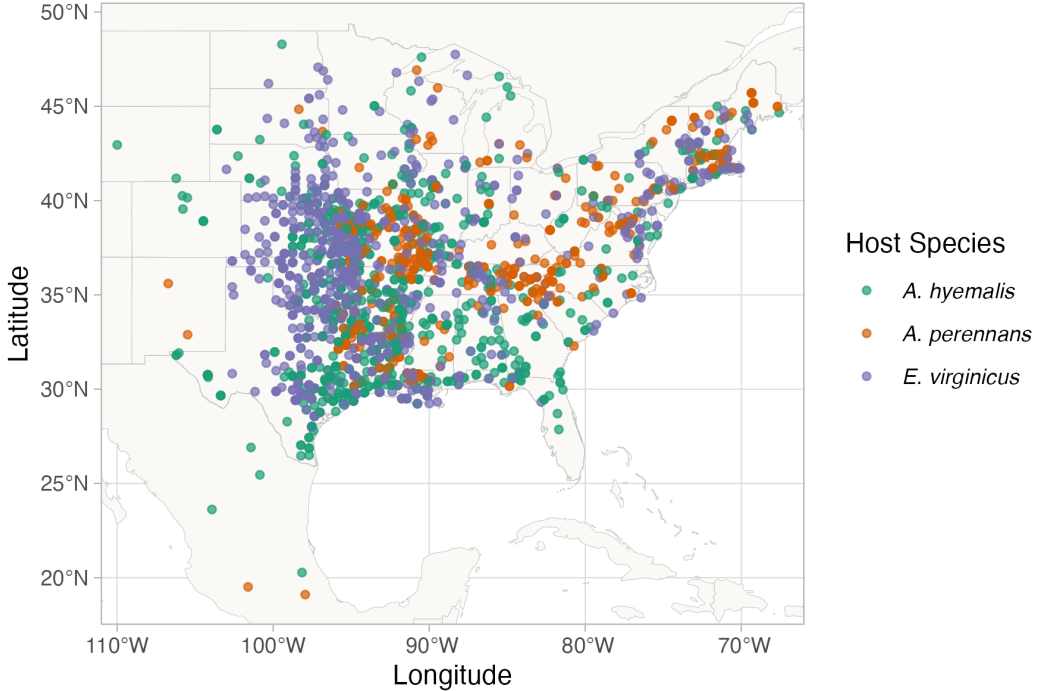


Figure 1: Collection locations of herbarium specimens sampled for *Epichloë* endophytes.

Specimens span eastern North America from nine herbaria, and are colored by host species (*A. hyemalis*: green, *A. perennans*: orange, *E. virginicus*: purple). Map lines delineate study areas and do not necessarily depict accepted national boundaries.

(INLA), to construct spatio-temporal models of endophyte prevalence. INLA provides a computationally efficient method of ascertaining parameter posterior distributions for certain models that can be formulated as latent Gaussian Models (Rue et al., 2009). Many common statistical models, including structured and unstructured mixed-effects models, can be represented as latent Gaussian Models. We incorporated spatial heterogeneity into this analysis using spatially-structured intercept and slope parameters implemented as stochastic partial differential equations (SPDE) to approximate a continuous spatial Gaussian process. This SPDE approach is a flexible method of smoothing across space while explicitly accounting for spatial dependence between data-points (Bakka et al., 2018; Lindgren et al., 2011). Fitting models with structured spatial effects is possible with MCMC sampling but can require long computation times, making INLA an effective alternative. This ap-

231 proach has been used to model spatial patterns in flowering phenology (Willems et al., 2022), the
232 abundance of birds (Meehan et al., 2019) and butterflies (Crossley et al., 2022), the distribution of
233 temperate trees (Engel et al., 2022) as well as the population dynamics of endangered amphibians
234 (Knapp et al., 2016) and other ecological processes (Beguin et al., 2012).

235 We estimated global and spatially-varying trends in endophyte prevalence using a joint-likelihood
236 model. For each host species h , endophyte presence/absence of the i^{th} specimen ($P_{h,i}$) was modeled
237 as a Bernoulli response variable with expected probability of endophyte occurrence $\hat{P}_{h,i}$. We mod-
238 eled $\hat{P}_{h,i}$ as a linear function of intercept A_h and slope T_h defining the global trend in endophyte
239 prevalence specific to each host species as well as with spatially-varying intercepts α_{h,l_i} and slopes
240 τ_{h,l_i} associated with location (l_i , the unique latitude-longitude combination of the i th observation).
241 The joint-model structure allowed us to “borrow information” across species in the estimation of
242 shared variance terms for the spatially-dependent random effect δ_{l_i} , intended to account for residual
243 spatial variation, and χ_{c_i} and ω_{s_i} , the i.i.d.-random effects indexed for each collector identity (c_i)
244 and scorer identity (s_i) of the i^{th} specimen.

$$\text{logit}(\hat{P}_{h,i}) = A_h + T_h * \text{year}_i + \alpha_{h,l_i} + \tau_{h,l_i} * \text{year}_i + \delta_{l_i} + \chi_{c_i} + \omega_{s_i} \quad (1)$$

245 By including random effects for collectors and scorers, we accounted for “nuisance” variance that
246 may bias predictions for changes in endophyte prevalence. Previous work suggests that behavior of
247 historical botanists may introduce biases into ecological inferences made from historic collections
248 (Kozlov et al., 2020). Prolific collectors who contribute thousands of specimens may be more or
249 less likely to collect certain species, or specimens with certain traits (Daru et al., 2018). Similarly,
250 the process of scoring seeds for hyphae involved multiple researchers (or "scorers") who, even with
251 standardized training, may vary in their likelihood of positively identifying *Epichloë*.

252 We performed model fitting using the inlabru R package (Bachl et al., 2019). Global intercept
253 and slope parameters, A and T , were given vague priors. Collector and scorer random effects, χ and
254 ω respectively, were centered at 0 with precision parameters assigned penalized complexity (PC)
255 priors with parameter values $U_{PC} = 1$ and $a_{PC} = 0.01$ (Simpson et al., 2017). Each spatially-

structured parameter depended on a covariance matrix according to the proximity of each pair of collection locations (Bakka et al., 2018; Lindgren et al., 2011). The covariance matrix was approximated using a Matérn covariance function, with each data point assigned a location according to the nodes of a mesh of non-overlapping triangles encompassing the study area (Fig. A2). Matérn covariance functions are widely used in spatial-statistical modeling because of their mathematical tractability and flexibility. This covariance structure relies on the assumption that the underlying process is stationary and isotropic, such that spatial autocorrelation between data points depends only on their relative positions (Bakka et al., 2018).

Implementing spatially-structured parameters in INLA with this SPDE approach is useful particularly because space is treated as a continuous variable, allowing the model to make efficient use of the data and generate predictions across the entire study region. The SPDE approach is flexible enough that it can capture smooth trends across space that are informed by the data rather than by spatial regions chosen *a priori* by researchers. However this flexibility also invites the risk of overfitting, as with other non-linear modeling approaches (Lapeyrolerie and Boettiger, 2023; Ramampiandra et al., 2023; Ward et al., 2014). Priors for the Matérn covariance function, termed "range" and "variance", define how proximity effects decay with distance. The choice of priors for these types of spatial models is an area of active research (Bakka et al., 2018; Simpson et al., 2017), but another advantage of the INLA approach is that its computational efficiency allows for sensitivity analyses. Results presented in the main text reflect a prior range of 342 kilometers (i.e. a 50% probability of estimating a range less than 342 kilometers). We tested a range of values (from 68 kilometers to 1714 kilometers) and meshes (presented in the Supporting Methods), finding that while the magnitude and uncertainty of effects varied, model results were qualitatively similar, i.e. the same direction of effects across space. We assessed model fit with visual posterior predictive checks (A3) and measurements of AUC (Figs. A4-A5) (Gelman and Hill, 2006). Through results and discussion that follow, we refer to the model described in this section as the “endophyte prevalence model”.

282

Modeling distributions of host species

283 The herbarium records did not encompass the entirety of each host species' range. Therefore, we
284 used additional data sources to model the geographic distribution of each host species, with two
285 goals: (1) generate realistic maps on which we could project the predictions of the INLA model,
286 and (2) use the geographic distributions to test for relationships between climate change drivers and
287 trends in endophyte prevalence. We followed the ODMAP (overview, data, model, assessment,
288 prediction) protocol (Crossley et al., 2022) (see Supporting Methods). In short, we used presence-
289 only observations of each host species from Global Biodiversity Information Facility (GBIF) between
290 1990 to 2020 (713 occurrence records for *A. hyemalis* (GBIF.Org, 2025a), 656 occurrence records
291 for *A. perennans* (GBIF.Org, 2025b), and 2338 occurrence records for *A. virginicus* (GBIF.Org,
292 2025c)). We fit maximum entropy (MaxEnt) models using the maxent function in the R package
293 dismo (Hijmans et al., 2017) using following seasonal climate predictors (1990-2020 climate normals):
294 mean and standard deviation of spring, summer, and autumn temperature, and mean and standard
295 deviation of spring, summer, and autumn cumulative precipitation. We generated 10,000 pseudo-
296 absences as background points, and split the occurrence data into 75% for model training and 25%
297 for model testing. The performance of models was evaluated with AUC (Jiménez-Valverde, 2012).
298 We found AUC values of 0.862, 0.838, 0.821 respectively for *Agrostis hyemalis*, *Agrostis perennans*,
299 and *Elymus virginicus* indicating good model fit to data. We used the training sensitivity (true
300 positive rate) and specificity (true negative rate) to set a threshold for transforming the continuous
301 predicted probabilities into binary presence - absence host distribution maps on which we projected
302 INLA predictions of endophyte prevalence (Liu et al., 2005).

303

Assessing the role of climate drivers

304 We assessed how the magnitude of climate change may have driven changes in endophyte prevalence
305 by assessing correlations between changes in climate and changes in endophyte prevalence predicted
306 from our spatial model at evenly spaced pixels across the study area.

307 We first downloaded monthly temperature and precipitation rasters from the PRISM climate
308 group (Daly and Bryant, 2013) covering the time period between 1895 and 2020 using the 'prism' R
309 package (Hart and Bell, 2015). Prism provides reconstructions of historic climate variables across
310 the United States by spatially interpolating weather station data (Di Luzio et al., 2008). Because
311 the magnitude of observed climate change differs across seasons, and because different growing
312 seasons is a key feature of the biology of our focal host species, we calculated 30-year climate
313 normals for seasonal mean temperature and cumulative precipitation for the recent (1990 to 2020)
314 and historic (1895 to 1925) periods. We used three four-month seasons within the year (Spring:
315 January, February, March, April; Summer: May, June, July, August; Autumn: September, October,
316 November, December). This division of seasons allowed us to quantify differences in the primary
317 climate change drivers, temperature and precipitation associated with the two "cool" seasons, when
318 we expected our focal species to be most active (*A. hyemalis* flowering phenology: spring; *E.
319 virginicus*: spring and summer; *A. perennans*: autumn). In addition to mean climate conditions,
320 environmental variability itself can influence population dynamics (Tuljapurkar, 1982) and changes
321 in variability are a key prediction of climate change models (IPCC, 2021; Stocker et al., 2013).
322 Therefore, we calculated the standard deviation for each annual and seasonal climate driver across
323 each 30-year period. We then took the difference between recent and historic periods for the
324 mean and standard deviation for each climate driver (Figs. A13-A15). All together, we assessed
325 twelve potential climate drivers: the mean and standard deviation of spring, summer, and autumn
326 temperature, as well as the mean and standard deviation of spring, summer, and autumn cumulative
327 precipitation (the same climate covariates used in the MaxEnt models).

328 We then evaluated whether areas that have experienced the greatest changes in endophyte preva-
329 lence (hotspots of endophyte change) are associated with high degrees of change in climate (hotspots
330 of climate change) To do so, we modeled the fitted, spatially-varying slopes of endophyte change
331 through time ($\tau_{[h]l}$) as a linear function of environmental covariates, with a Gaussian error distri-
332 bution for a set of pixels across each host distribution. The continuous SPDE approach taken from
333 our endophyte prevalence model allows us to generate predictions of temporal trends in prevalence

334 at arbitrarily many pixels across each host distribution. Balancing computation time with resolu-
335 tion, we generated predicted trends for 546, 645, and 753 pixels across each host distribution for *A.*
336 *perennans*, *A. hyemalis*, and *E. virginicus* respectively (pixel dimensions: *A. perennans* = 65 km
337 x 36 km; *A. hyemalis* = 61km x 45 km; *E. virginicus* = 62 km x 40 km). Fitting regressions to
338 many pixels across the study region risks artificially inflating confidence in our results due to large
339 sample sizes, and so we performed this analysis using only a random subsample of 250 pixels across
340 the study region; other sizes of subsample yielded similar results. Data from each host species were
341 analyzed separately. Throughout the results and discussion that follow, we refer to this analysis as
342 the “*post hoc* climate regression analysis”.

343 *Validating model performance with in-sample and out-of-sample tests*

344 We evaluated the predictive ability of the endophyte prevalence model using both in-sample train-
345 ing data from the herbarium surveys, and with out-of-sample test data, an important but rarely
346 used strategy in ecological studies (Lee et al., 2024; Tredennick et al., 2021). We generated out-of-
347 sample test data from contemporary surveys of endophyte prevalence in natural populations of *A.*
348 *hyemalis* and *E. virginicus* in Texas and the southern US. Surveys of *E. virginicus* were conducted
349 in 2013 as described in Sneck et al. (2017), and surveys of *A. hyemalis* took place between 2015 and
350 2020. Population surveys of *A. hyemalis* were initially designed to cover longitudinal variation in
351 endophyte prevalence towards its range edge, while surveys of *E. virginicus* were designed to cover
352 latitudinal variation. In total, we visited 43 populations of *A. hyemalis* and 20 populations of *E.*
353 *virginicus* across the south-central US, with emphasis on Texas and neighboring states (Fig A12).
354 During surveys, we collected seeds from up to 30 individuals per population (average number of
355 plants sampled per population: 22.9); note that this sampling design provided greater local depth
356 of information than the herbarium records, where only one plant was sampled at each locality. We
357 quantified the endophyte status of each individual with microscopy as described for the herbarium
358 surveys (with 5-10 seeds scored per individual), and calculated the prevalence of endophytes within
359 the population (proportion of plants that were endophyte-symbiotic). For each population, we com-

360 pared the observed fraction of endophyte-symbiotic hosts to the predicted probability of endophyte
361 occurrence \hat{P} derived from the model for that location and year. The contemporary survey period
362 (2013–2020) is at the most recent edge of the time period encompassed by the historical specimens
363 used for model fitting.

364

Results

365 *How has endophyte prevalence changed over time?*

366 Across more than 2300 herbarium specimens dating back to 1824, we found that prevalence of
367 *Epichloë* endophytes increased over the last two centuries for all three grass host species (Fig. 2).
368 On average, endophytes of *A. perennans* and *E. virginicus* increased from ~ 40 % to 70% prevalence
369 across the study region, and *A. hyemalis* increased from ~ 25% to over 50% prevalence. Our model
370 indicates high confidence that overall temporal trends are positive across species (99% probability
371 of a positive overall year slope in *A. hyemalis*, 92% probability of a positive overall year slope in *A.*
372 *perennans*, and 91% probability of a positive overall year slope in *E. virginicus*) (Fig. A6).

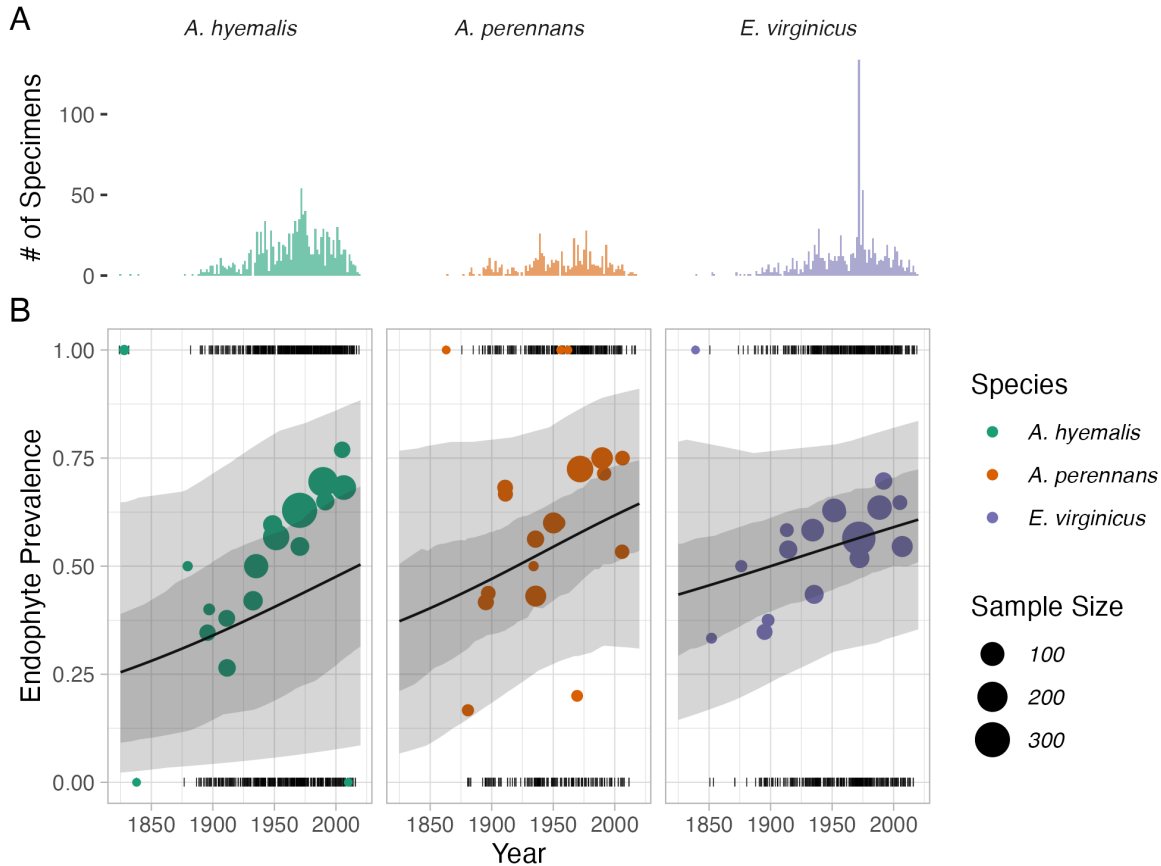


Figure 2: **Temporal trends in endophyte prevalence.** (A) Histograms show the frequency of scored specimens through time for each host species. (B) Lines show mean endophyte prevalence predicted by the endophyte prevalence model over the study period along with the 50% and 95% CI bands incorporating parameter uncertainty and variation associated with collector and scorer random effects. Colored points are binned means of the observed endophyte presence/absence data (black dashes). Colors represent each host species (*A. hyemalis*: green, *A. perennans*: orange, *E. virginicus*: purple) and point size represents the number of specimens.

373 The model appears to under-predict the observed increase in endophyte prevalence relative to
 374 the data, particularly for *A. hyemalis* (Fig. 2B), but the model is accounting for random effects
 375 and spatial non-independence that are not readily seen in the figure. We found no evidence that
 376 collector biases influenced our results. Collector random effects were consistently small (Fig. A9),

377 and models fit with and without this random effect provide qualitatively similar results. The identity
378 of individual scorers, the researchers who identified endophyte status microscopically, did contribute
379 to observed patterns in endophyte prevalence. For example, 3 of the 25 scorers were significantly
380 more likely than average to assign positive endophyte status, as indicated by 95% credible intervals
381 greater than zero, while 4 of the 25 had 95% credible intervals below zero (Fig. A10).

382 *How spatially variable are temporal trends in endophyte prevalence?*

383 While there was an overall increase in endophyte prevalence, our model revealed hotspots and
384 coldspots of change across the host species' ranges, which are mapped in Fig. 3 across geographic
385 ranges predicted by MaxEnt species distribution models. In some regions, posterior mean esti-
386 mates of spatially varying temporal trends indicate that *A. hyemalis* and *A. perennans* experienced
387 increases in prevalence by as much as 2% per year over the study period, while *E. virginicus* ex-
388 perienced increases up to around 1% per year. Both *Agrostis* species show areas of strong increase
389 and areas of declining prevalence, while *E. virginicus* had an overall weaker and geographically
390 more homogeneous increase in endophyte prevalence. Notably, endophytes are predicted to have
391 increased most strongly towards the western range edge of *A. hyemalis* (Fig. 3A) and across the
392 northeastern US for *A. perennans* (Fig. 3B). Broad increases in prevalence on average, along with
393 increases towards range edges that had low historic prevalence result in range expansions of the
394 symbiosis for both *Agrostis* species (Fig. 4). Increases in prevalence were strongest in regions with
395 low historic prevalence for the *Agrostis* species (Fig. A11 A-B), but for *E. virginicus* trends did
396 not differ according to historic prevalence (A11 C). Posterior estimates of uncertainty in spatially
397 varying slopes indicate that these hotspots of change may have experienced increases of up to 5%
398 per year while declines in prevalence may be as great as -4% per year for *A. hyemalis* and *A.*
399 *perennans*. For *E. virginicus*, uncertainty ranges between 3.5% increases and 2.5% decreases (Fig.
400 A7).

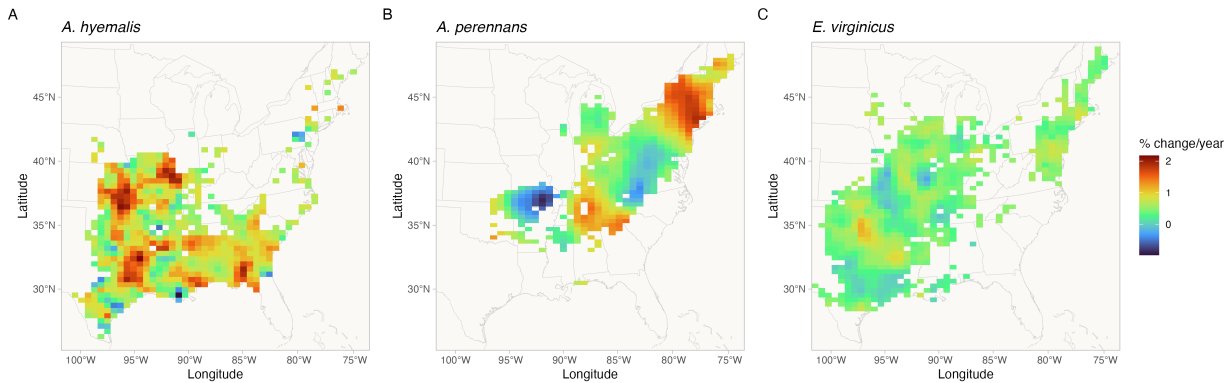


Figure 3: Predicted posterior mean of spatially-varying slopes representing change in endophyte prevalence for each host species (A, *A. hyemalis*; B, *A. perennans*; C, *E. virginicus*). Spatially-varying trends are estimated from the endophyte prevalence model. Color indicates the relative change in predicted endophyte prevalence. Map lines delineate study areas and do not necessarily depict accepted national boundaries.

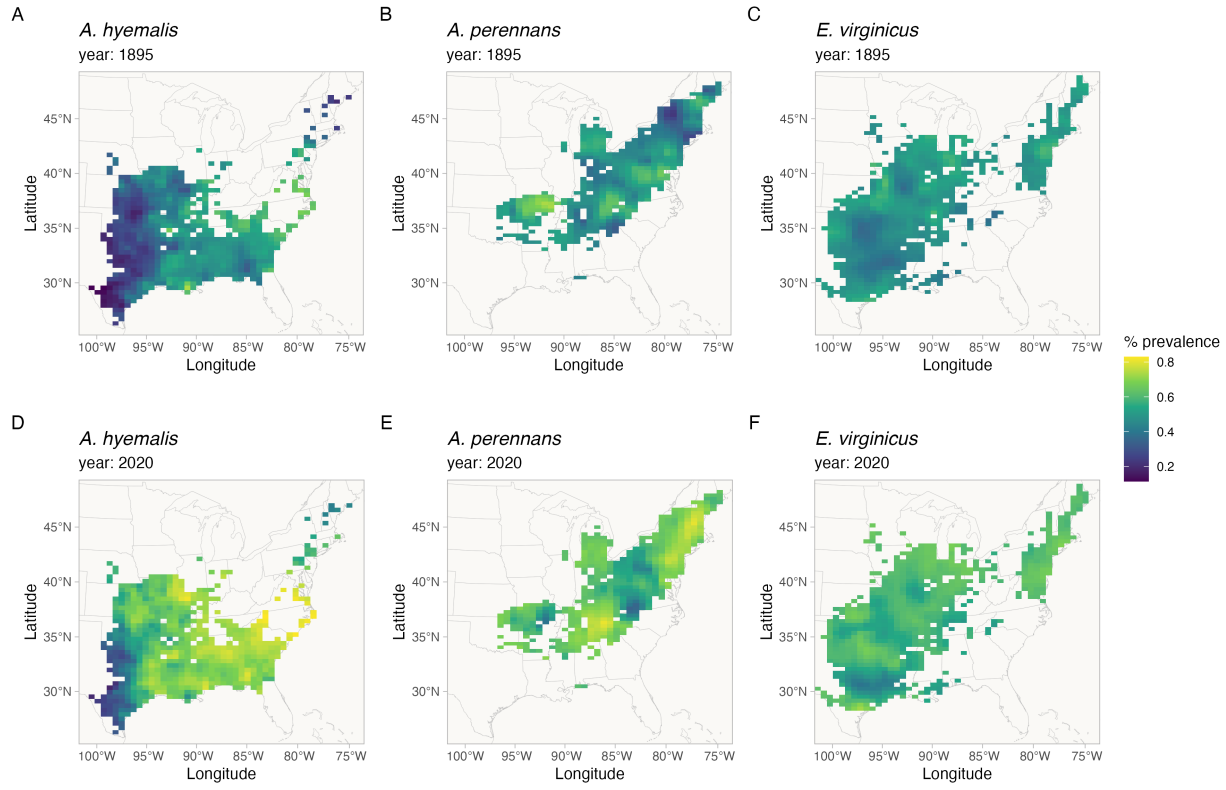


Figure 4: Predicted endophyte prevalence for each host species in 1895 and 2020. Predictions of prevalence come from the endophyte prevalence model. Color indicates the posterior mean endophyte prevalence for *A. hyemalis* (A,D), *A. perennans* (B,E), and *E. virginicus* (C,F). Map lines delineate study areas and do not necessarily depict accepted national boundaries.

401 *What is the relationship between variation in temporal trends in endophyte
402 prevalence and changes in climate drivers?*

403 We found that trends in endophyte prevalence were strongly associated with one or more seasonal
404 climate change drivers (Fig. 5). For the majority of the study region, the climate has become wetter
405 (an average increase in annual precipitation of 60 mm) with relatively little temperature warming
406 (an average increase in annual temperature of 0.02 °C) over the last century (Fig. A13-A15), a
407 consequence of regional variation in global climate change (IPCC, 2021). Within the region, climate

408 changes were spatially variable; certain locations experienced increases in annual precipitation as
409 large as 375 mm or decreases up to 54 mm across the last century, while annual temperature changes
410 ranged from warming as great as 1.4 °C to cooling by 0.46 °C. Spatially variable climate trends were
411 predictive of trends in endophyte prevalence. For example, strong increases in endophyte prevalence
412 for *A. perennans* were most strongly associated with increasing autumn precipitation and with
413 increasing mean and variability in autumn temperature (greater than 97% posterior probabilities
414 of positive slopes). For this species, each 1 °C increase in autumn temperature was associated with
415 a 1.07 % greater increase per year in endophyte prevalence (Fig. 5A) and a 100 mm increase in
416 precipitation was associated with a 0.8% greater increase per year in endophyte prevalence (Fig.
417 5B). This result aligns with the species' autumn active growing season, however other seasonal
418 climate drivers were also associated with increasing endophyte prevalence in this host species. In
419 particular, we found cooler and drier springs and cooler summers to be associated with increasing
420 endophyte prevalence (greater than 99% posterior probabilities of negative slopes), though these
421 slopes were generally of smaller magnitude than those for autumn climate drivers.

422 Changes in endophyte prevalence across the ranges of *A. hyemalis* and *E. virginicus* were less
423 strongly driven by changes in climate. Like *A. perennans*, climate during peak growing season
424 (spring for *A. perennans* and summer for *E. virginicus*) emerged most commonly as drivers of
425 changes in endophyte prevalence. Increases in mean spring precipitation were the strongest predictor
426 of increasing trends in endophyte prevalence for *A. hyemalis* (Fig. 5B) (greater than 99% posterior
427 probability of a positive slope). For this species, an increase of 100 mm in spring precipitation was
428 associated with 0.6% per year stronger increases in endophyte prevalence relative to regions with
429 no change in precipitation. The next greatest slopes were those associated with variability in spring
430 precipitation (greater than 96% posterior probability of a negative slope), as well as in the mean
431 and variability of autumn climate (greater than 98% probability of negative and positive slopes,
432 respectively). Changes in endophyte prevalence in *E. virginicus* were not strongly associated with
433 changes in most climate drivers, but regions with reduced variability in autumn precipitation (Fig.
434 5B) and with cooler and more variable summer temperatures (Fig. 5A,C) experienced the largest

435 increases in endophyte prevalence. Our analysis indicated relatively high confidence that these
436 climate drivers influence endophyte prevalence shifts in *E. virginicus*(greater than 99% posterior
437 probability of either negative or positive slopes respectively), however they translate, for example,
438 to less than a 0.4% decrease in endophyte prevalence per year for each 1°C of summer warming
439 over the century. Repeating this analysis using all pixels across each species' distribution were
440 qualitatively similar to these results.

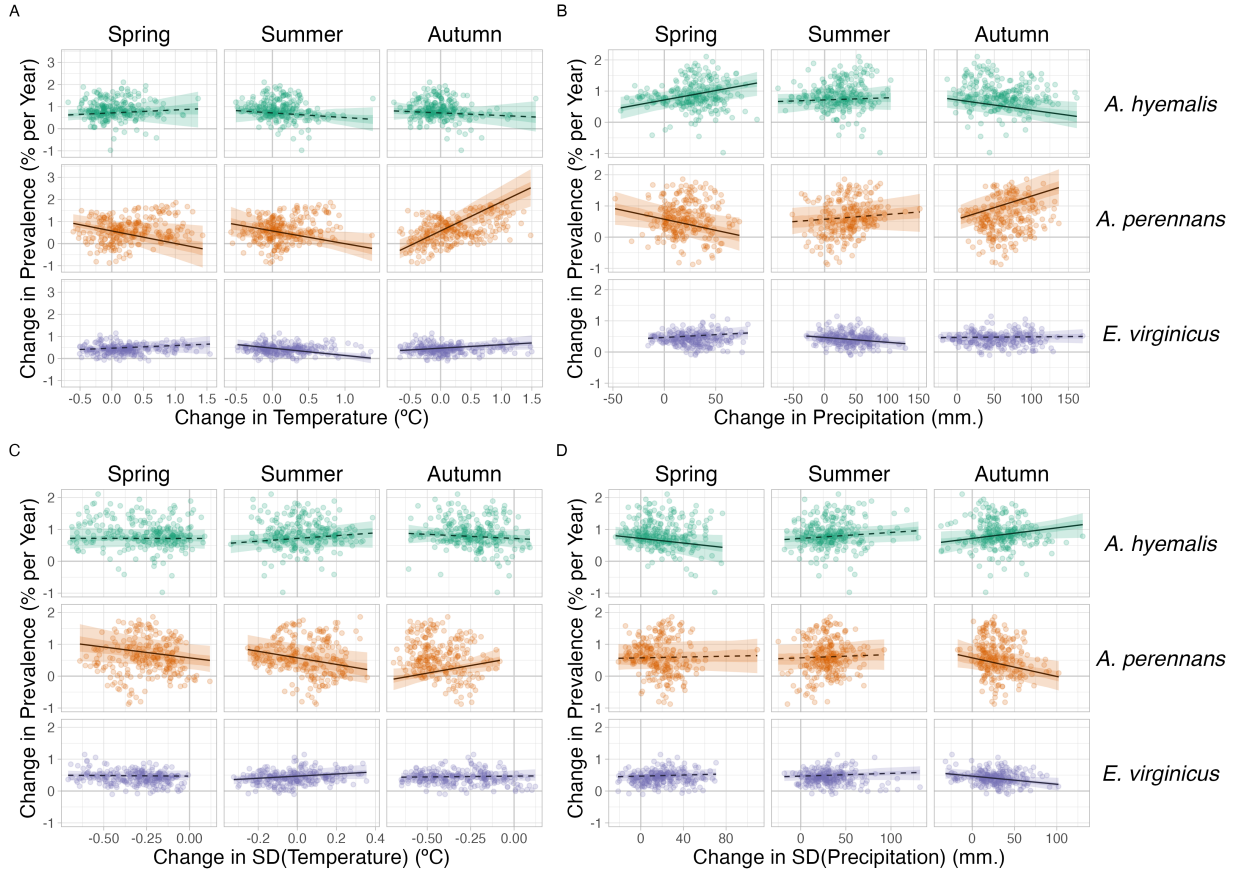


Figure 5: Relationships between predicted trends in endophyte prevalence and changes in seasonal climate drivers. Lines show marginal predicted relationship between spatially-varying trends in endophyte prevalence and changes in mean and variability of climate ((A): mean temperature, (B): cumulative precipitation, (C): standard deviation in temperature, (D): standard deviation in precipitation) estimated from the *post hoc* climate regression analysis. Confidence bands represent the 50 and 95% CI, colored by host species (*A. hyemalis*: green, *A. perennans*: orange, *E. virginicus*: purple). Slopes with greater than 95% posterior probability of being either positive or negative are represented as solid lines while those that have less than 95% probability are dashed. Points are the values of pre-computed SVC trends and climate drivers at 250 randomly sampled pixels across each host's distribution used in model fitting for the *post hoc* climate regression analysis.

441

Evaluation of model performance on an out-of-sample test

442 Tests of the endophyte prevalence model's predictive performance as quantified by AUC and by
443 visual posterior predictive checks, indicated good predictive ability. Model performance was similar
444 between historic herbarium specimens used as training data and the out-of-sample test data from
445 contemporary surveys (AUC = 0.79 and 0.77 respectively; Fig. A5-A4). The model successfully
446 captured broad regional trends in endophyte prevalence seen in the contemporary survey data,
447 such as decline endophyte prevalence in *A. hyemalis* towards western longitudes (Fig. 6A) and an
448 increase towards northern latitudes (Fig. 6B). It is noteable that model predictions for endophyte
449 prevalence exhibited relatively little local geographic variation, whereas the out-of-sample survey
450 data were highly variable with populations spanning 0% to 100% endophyte-symbiotic plants (Fig.
451 6C), indicating population-to-population variation not captured in the endophyte prevalence model.

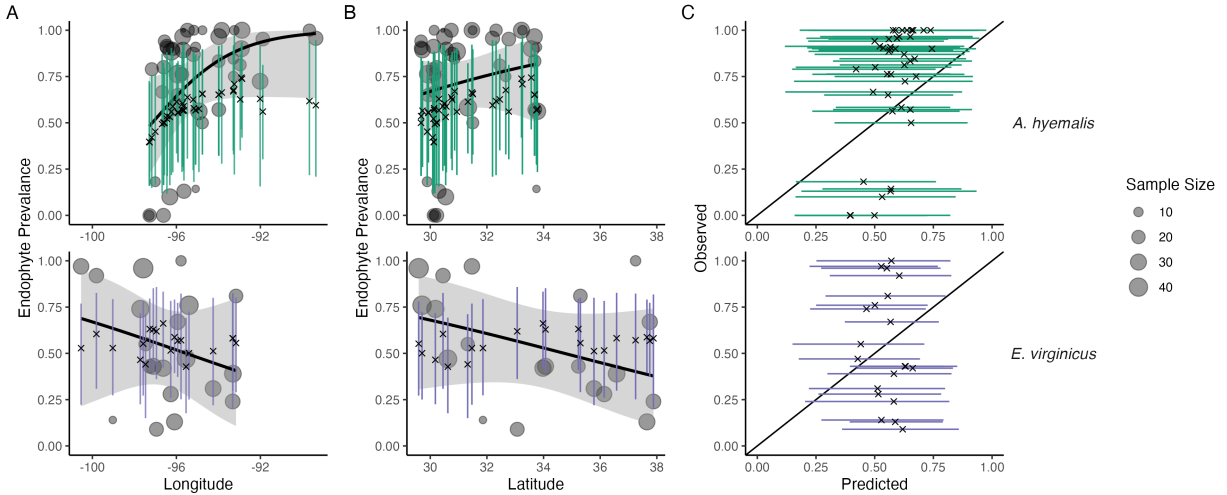


Figure 6: **Predictive performance for contemporary test data.** (A) The endophyte prevalence model, trained on historic herbarium collection data, performed modestly at predicting prevalence in contemporary population surveys. The model captured regional trends across (A) longitude and (B) latitude. Crosses indicate predicted mean prevalence along with the 95% CI (colored lines: *A. hyemalis*: green, orange, *E. virginicus*: purple) from the herbarium model. Contemporary prevalence is represented by grey points (point size reflects sample size) along with trend lines from generalized linear models (black line and shaded 95% confidence interval). (C) Comparison of contemporary observed population prevalence vs. predicted endophyte prevalence shows that contemporary test data had more variance between populations than in model predictions.

Discussion

Our examination of historic plant specimens revealed previously hidden shifts in microbial symbiosis over the last two centuries. For the three grass host species we examined, there have been strong increases in prevalence of *Epichloë* endophyte symbiosis. We interpret increases in prevalence of *Epichloë*, which are vertically transmitted, as adaptive changes that improve the fitness of their hosts under increasing environmental stress. This interpretation is in line with theory predicting that positive fitness feedback caused by vertical transmission leads beneficial symbionts to rise in

459 prevalence within a population (Donald et al., 2021; Fine, 1975). We further found that trends
460 in endophyte prevalence varied across the distribution of each species in association with changes
461 in climate drivers, suggesting that the increases in endophyte prevalence are driven by context-
462 dependent benefits to hosts that confer resilience under environmental change. Taken together, this
463 suggests an overall strengthening of host-symbiont mutualism over the last two centuries.

464 *Responses of host-microbe symbioses to climate change*

465 Differences across host species underscore that while all of these C_3 grasses share similar broad-scale
466 distributions, each engages in unique biotic interactions and has unique responses to environmental
467 drivers. We identified hotspots of change for *A. perennans*, which was the species whose endophyte
468 prevalence was most responsive to changes in climate drivers (Fig. 5). Predicted declines of 0.9%
469 per year in the southern portion of its range and predicted increases of up to 2% per year in the
470 north suggest a potential poleward range shift of endophyte-symbiotic plants (Fig. 3B); whether
471 the overall host distribution is shifting in parallel is an exciting next question.

472 Based on previous work demonstrating that endophytes can shield their hosts from drought
473 stress (reviewed in Decunta et al. (2021)), we generally predicted that drought conditions would be
474 a driver of increasing endophyte prevalence. In contrast to this expectation, increasing prevalence
475 for *A. perennans* was associated with both increasing autumn temperature and precipitation (Fig.
476 5). To our knowledge, the response of the symbiosis in *A. perennans* to drought has not been
477 examined experimentally, but in a greenhouse experiment, endophytes had a positive effect on host
478 reproduction under shaded, low-light conditions (Davitt et al., 2010). Our results also hint that it
479 may be useful to investigate whether lagged climate effects are important predictors of host fitness
480 in this system (Evers et al., 2021). Endophyte prevalence of the autumn-flowering *A. perennans* was
481 strongly linked with decreasing spring precipitation, and that of the spring-flowering *A. hyemalis*
482 was associated with decreasing autumn precipitation (Fig. 5B). For *A. hyemalis*, endophytes could
483 be playing a role helping hosts weather autumn-season droughts, which is likely also an important
484 time for the species' germination. Previous work demonstrated drought benefits in a greenhouse

manipulation with this host-symbiont pair (Davitt et al., 2011), and early life stages may be particularly vulnerable to prolonged droughts. For *E. virginicus*, which experienced the weakest changes in endophyte prevalence overall (ranging between 1.1% increases and 0.2% decreases), we only found modest associations with changes in climate drivers. Surveys by Sneck et al. (2017), used as part of the test data in this study, identified a drought index (SPEI) that integrates precipitation with estimated evapotranspiration as an important predictor of contemporary endophyte prevalence in this species. The diverse relationships we detect between trends in endophyte prevalence and climate drivers suggest a more complicated picture than the simple explanation that drought alone, as measured through changes in annual precipitation, causes increasing endophyte prevalence through context-dependent fitness benefits.

While we show consistent increasing trends in prevalence between the three species, the mechanisms that explain these changes may be diverse and idiosyncratic. First, climate change responses may depend on genotype-specific responses that are not considered in our current analysis. While *Epichloë* symbioses are highly specialized, surveys have demonstrated genotypic and chemotypic diversity of the symbionts among and within populations (Treindl et al., 2023; von Cräutlein et al., 2021). Genotypic variation in *Epichloë* endophytes, particularly in genes responsible for alkaloid production, produces "chemotypes" with differing benefits for hosts against insect or mammalian herbivores mediated by environmental conditions (Saikkonen et al., 2013; Schardl et al., 2012). Genotypic variation of the hosts themselves can also influence interaction outcomes (Gundel et al., 2011; Parker et al., 2017). Whether hotspots of change in endophyte prevalence reflect selection for genotype-pairings with particularly strong fitness benefits is an unanswered question. Additionally, *Epichloë* endophytes have been connected to a suite of non-drought related fitness benefits including herbivory defense (Brem and Leuchtmann, 2001), salinity resistance (Wang et al., 2020), and mediation of pathogens (Vikuk et al., 2019) and the soil microbiome (Roberts and Ferraro, 2015). Broad changes in the distribution and abundance of natural enemies (Côté et al., 2004), along with stresses from anthropogenic changes in land management and pollution (Sage, 2020) likely influence the benefits of symbiosis (Rudgers et al., 2020). Host species experience a world that is made

512 increasingly stressful by the combination of these global change drivers, and while historic trends
513 that we observed suggest that symbiotic fitness benefits have helped mitigate this stress, it is likely
514 that at some higher leveler of stress, increasing costs of maintaining the mutualism could lead to
515 declines in endophyte prevalence. Changing endophyte prevalence results from the combination of
516 net fitness benefits playing out across the heterogeneous map of a changing climate and and its
517 interactive effects on other anthropogenic drivers.

518 Our results indicate that *Epichloë* symbiosis has likely improved host fitness in stressful en-
519 vironments leading to increasing prevalence. What is less clear is how this will influence future
520 range shifts. Based on our analysis, it is likely that the symbiosis will facilitate range shifts for
521 hosts by improving population growth at range edges. Previous population surveys (Rudgers and
522 Swafford, 2009; Semmarin et al., 2015; Sneck et al., 2017) attributed environment-dependent gra-
523 dients in endophyte prevalence to symbiont-derived fitness benefit's allowing hosts to persist in
524 environments where they otherwise could not (Afkhami et al., 2014; Kazenel et al., 2015). However,
525 symbiont-facilitated range shifts require that endophytes be present in the populations to be able
526 to contribute to population growth. The arid western range edge of *A. hyemalis* has had histor-
527 ically low endophyte prevalence (Fig. 4), and while prevalence has increased most quickly in the
528 regions with historically low endophyte prevalence (Fig. A11), the complete absence of endophytes
529 at range edges in this species would make it impossible for prevalence to increase without dispersal
530 of symbiotic seeds (Fowler et al., 2023). These factors potentially contribute to the ability of the
531 host species to track its environmental niche. Another interesting question is the degree to which
532 symbiotic and non-symbiotic hosts, which occupy overlapping but distinct niches, are likely to ex-
533 perience distribution shifts in tandem or at different rates in future. More extreme climate stresses,
534 which are expected more frequently in the future (Seneviratne et al., 2021), have the potential to
535 alter the costs and benefits of the interaction. The past indicates a resilient symbiosis, but it will
536 be crucial to understand whether more extreme future climate conditions could tip this interaction
537 to deteriorate.

538 *Steps towards forecasts of host-microbe symbioses*

539 The combination of a spatially-explicit model and historic herbarium specimens allowed us to
540 identify regions of both increasing and decreasing endophyte prevalence, however we see several
541 next steps toward the goal of predicting host and symbiont niche-shifts in response to future cli-
542 mate change. While the model recreated the large-scale spatial trends observed in contemporary
543 population surveys, test data contained more population-to-population variability in prevalence than
544 could be explained by the model. We interpret this to mean that the model captures coarse-scale
545 spatial and temporal trends reasonably well, but is not equipped to capture local-scale nuances that
546 generate population-to-population differences. Validating our model predictions with this test, a
547 rare extra step in collections-based studies, allows us to identify ways in which the model's out-of-
548 sample predictive ability could be improved. Lack of information on local variability in symbiont
549 prevalence may simply be a feature of data derived from herbarium specimens. Natural history
550 collectors sample one or a few specimens from local populations, and these observations are aggre-
551 gated by the model to derive broad-scale estimates. This suggests that increasing local replication
552 should be a factor considered in future collection efforts of natural history specimens, balancing the
553 required time and effort along with limitations on storage space within collections. An alternative
554 validation test would be to hold-out samples from within the historic data set. Such a test would
555 more clearly provide a set of data that matched the conditions of the training data (i.e in spatial
556 scale and climate conditions) missing within the contemporary test data, however a relatively lim-
557 ited number of sampled specimens held us back from exploring this option. Splitting datasets can
558 negatively impact model estimates, and the choice of how to split the data for model validation is
559 not trivial (Bergmeir and Benítez, 2012; James et al., 2013). From a modeler's perspective, this
560 also urges advocacy for increased collection efforts and expansion of herbarium collections.

561 Another key consideration in forecasting the dynamics host-microbe symbioses is the spatial
562 scale of both specimen georeferencing and available climate data. For this analysis, most specimen
563 localities were assigned coordinates at county or city centroids, and the climate data examined

564 was on 4 km grid cells. Georeferencing of specimens as accurately as possible is a key priority
565 of herbarium specimen digitization efforts (Davis, 2023; Soltis, 2017). While the INLA modeling
566 approach that we used allows for predictions at arbitrarily small spatial scales, and would simplify
567 connecting model predictions to the scale of a given climate driver, the coarse scale inherent to our
568 analysis may obscure some local-scale ecological processes. Poor predictive ability at local scales in
569 this grass-endophyte system is not surprising, as previous studies have found that local variation,
570 even to the scale of hundreds of meters can structure endophyte-host niches (Gundel et al., 2024;
571 Kazenel et al., 2015). An important step would be integrating data from local and regional scales
572 through modeling to constrain estimates of local and regional variation.

573 Predicting future niche-shifts of hosts and symbionts will require considering the coupled dynam-
574 ics of host-symbiont dispersal in addition to fitness benefits. For example, transplanting symbiotic
575 and non-symbiotic plants beyond the range edge of *A. hyemalis* could tell us whether low endophyte
576 prevalence in that area (Fig. 4A) is a result of environmental conditions that lead the symbiosis
577 to have negative fitness consequences, or is a result of some historical contingency or dispersal lim-
578 itation that has thus far limited the presence of symbiotic hosts from a region where they would
579 otherwise flourish and provide resilience. Another interesting question is whether local adaption,
580 in either host or symbiont may influence future range shifts. Incorporating available climatic and
581 soil layers as covariates is another obvious step that could improve predictions. These steps will
582 bridge gaps that often exist between large but broad bioclimatic and biodiversity data and small but
583 high-resolution data on biotic interactions, and move towards the goal of predicting the dynamics
584 of microbial symbioses under climate change (Isaac et al., 2020; Miller et al., 2019).

585 *Herbaria for global change research*

586 Our analysis advances the use of herbarium specimens in global change biology in two ways.
587 First and foremost, this is one of a growing number of studies to examine microbial symbiosis using
588 specimens from natural history collections, and the first, to our knowledge, to link long-term changes
589 in the symbioses to changes in climate. The responses of microbial symbioses are a rich target for
590 future studies within historic specimens, particularly those that take advantage of advances in

sequencing technology. While we used relatively coarse presence/absence data based on fungal morphology, other studies have examined historic plant microbiomes using molecular sequencing and sophisticated bioinformatics techniques, but these studies have so far been limited to relatively few specimens at limited spatial extents (Bearchell et al., 2005; Bieker et al., 2020; Bradshaw et al., 2021, 2023; Gross et al., 2021; Heberling and Burke, 2019; Yoshida et al., 2015). Much of this work highlights the important role that historic specimens can play in tracking pathogens, a particularly important area as climate change facilitates the spread of new diseases (Ristaino, 2020; Singh et al., 2023) Continued advances in capturing historic DNA and in filtering out potential contamination during specimen storage (Bakker et al., 2020; Daru et al., 2019; Raxworthy and Smith, 2021) will be imperative in the effort to scale up these efforts. This scaling up will be essential to be able to quantify changes not just in the prevalence of symbionts, but also in symbionts' intraspecific variation and evolutionary responses to climate change, as well as in changes in the wider host microbiome. With improved molecular insights from historic specimens, we could ask whether the broad increases in endophytes that we have identified reflect selection for particular genetic strains or chemotypes and how this selection varies across space. Answering these questions as well as the unknown questions that future researchers may ask also reiterates the value in capturing meta-information during ongoing digitization efforts at herbaria around the world and during the accession of newly collected specimens (Edwards et al.; Lendemer et al., 2020).

The second major advance in this analysis is in accounting for several potential biases in the data observation process that may be common to many collections-based research questions by using a spatially-explicit random effects model. Potential biases introduced by the sampling habits of collectors (Daru et al., 2018), and variation between contemporary researchers during the collection of trait data, if not corrected for could lead to over-confident inference about the strength and direction of historic change (Fig. 2). Previous studies that have quantified the effects of collector biases typically find them to be small (Davis et al., 2015; Meineke et al., 2019), and we similarly did not find that collector has a strong effect on the results of our analysis, but that scorer identity did impact results. It is difficult to distinguish whether the impact of scorers was driven by true differences

618 in scorers' biases or by unintended spatial or temporal clustering of the specimens examined by
619 each scorer (Clayton et al., 1993; Urdangarin et al., 2023). By under-weighting endophyte-positive
620 samples that are clustered spatially or by collector or observer, the endophyte prevalence model is
621 appropriately accounting for nuisance variables and providing a conservative inference of endophyte
622 change relative to the raw data. Spatial autocorrelation is another phenomenon likely common in
623 data derived from herbarium specimens (Willems et al., 2022), which our spatially-explicit analysis
624 models among samples. Beyond spatial autocorrelation of outcomes, systematic differences in sam-
625 pling across space can result in spatial bias. One strength of herbaria as vehicles for global change
626 research is the relative ease with which specimens from many distinct geographic locations can be
627 examined. We visited just nine institutions in the central southern United States, and we were able
628 to sample seeds from specimens across an area spanning over 300,000 sq. km, including specimens
629 from Mexico and Canada. Despite this advantage, the specimens we examined are concentrated in
630 the south-central United States, with fewer specimens in the rapidly warming northeastern United
631 States reflecting the regional focus of herbaria. We provide a simulation analysis exploring the
632 potential impact of spatially and temporally biased sampling (Appendix A - Supporting Methods).
633 We found that the spatially-varying coefficient model had a strong ability to re-capitulate temporal
634 trends across space in simulated data, and that this result was robust to relatively high levels of
635 spatial bias (80% of data missing from one spatial region). Simulation analyses that extend this
636 work to consider the myriad ways herbarium data may be biased (i.e. testing different spatial ar-
637 rangements and scales of spatial bias, or testing different sample sizes) would be extremely valuable
638 (Daru et al., 2018; Erickson and Smith, 2021; Gaul et al., 2020; Meineke and Daru, 2021; Schmidt
639 et al.).

640 Conclusion

641 Ultimately, a central goal of global change biology is to generate predictive insights into the future of
642 natural systems on a rapidly changing planet. Beyond host-microbe symbioses, detecting ecological
643 responses to anthropogenic global change and attributing their causes would inform public policy
644 decision-makers and adaptive management strategies. Natural history specimens, such as the plant

645 hosts examined in this study have a clear role to play in informing global change biodiversity science,
646 including building understanding of the dynamics of host-symbiont interactions (Davis, 2023). This
647 survey of historic endophyte prevalence is necessarily correlative, yet it serves as a foundation to
648 develop better predictive models of the response of microbial symbioses to climate change. By
649 comparing detected ecological responses with alternative mechanistic simulations of the past, we
650 could attribute their cause, in a manner similar to methods from climate science and economics
651 (Carleton and Hsiang, 2016; Stott et al., 2010; Trenberth et al., 2015). Combining the insights from
652 this type of regional-scale survey with field experiments and physiological performance data could be
653 invaluable to identify mechanisms driving shifts in host-symbiont dynamics. Evidence is strong that
654 certain dimensions of climate change correlated with endophytes' temporal responses, however we
655 do not know why trends in prevalence were weak in some areas or how endophytes would respond
656 to more extreme changes in climate. The "time machine" of natural history collections revealed
657 evidence of mutualism resilience for grass-endophyte symbioses in the face of environmental change,
658 but more extreme changes could potentially push one or both partners beyond their physiological
659 limits, leading to the collapse of the mutualism; more research is needed to understand what those
660 limits might be.

661 Acknowledgments

662 We thank Dr. Jessica Budke for help in drafting our initial destructive sampling plan, and to the
663 many staff members of herbaria who facilitated our research visits, as well as to the hundreds of
664 collectors who contributed to the natural history collections. Several high school and undergraduate
665 researchers contributed to data collection, including A. Appio-Riley, P. Bilderback, E. Chong, K.
666 Dickens, L. Dufresne, B. Gutierrez, A. Johnson, S. Linder, E. Scales, B. Scherick, K. Schrader, E.
667 Segal , G. Singla, and M. Tucker. This research was supported by funding from National Science
668 Foundation (grants 1754468 and 2208857) and by funding from the Texas Ecolab Program. Two
669 anonymous reviewers greatly improved an earlier version of this manuscript.

670

Statement of Authorship

671 J.C.F. contributed to research conception, data collection, data analysis, and led manuscript draft-
672 ing. J.M. contributed to data analysis and manuscript revisions. T.E.X.M. contributed to research
673 conception, data collection, data analysis, and manuscript revisions.

674

Data and Code Availability

675 Data from this publication can be found through a publicly available repository
676 (<https://doi.org/10.5061/dryad.rn8pk0pn0>). Code for analyses can be found through a publicly
677 available repository (<https://github.com/joshuacfowler/EndoHerbarium>) that will be permanently
678 archived upon publication.

Literature Cited

- 680 M E Afkhami. Fungal endophyte–grass symbioses are rare in the California floristic province and
681 other regions with mediterranean-influenced climates. *Fungal Ecology*, 5(3):345–352, 2012.
- 682 M E Afkhami and J A Rudgers. Symbiosis lost: Imperfect vertical transmission of fungal endophytes
683 in grasses. *The American Naturalist*, 172(3):405–416, 2008.
- 684 M E Afkhami, P J McIntyre, and S Y Strauss. Mutualist-mediated effects on species’ range limits
685 across large geographic scales. *Ecology Letters*, 17(10):1265–1273, 2014.
- 686 S N Aitken, S Yeaman, J A Holliday, T Wang, and S Curtis-McLane. Adaptation, migration
687 or extirpation: Climate change outcomes for tree populations. *Evolutionary Applications*, 1(1):
688 95–111, 2008.
- 689 C E Aslan, E S Zavaleta, B Tershy, and D Croll. Mutualism disruption threatens global plant
690 biodiversity: a systematic review. *PloS one*, 8(6):e66993, 2013.
- 691 F E Bachl, F Lindgren, D L Borchers, and J B Illian. inlabru: an R package for Bayesian spatial
692 modelling from ecological survey data. *Methods in Ecology and Evolution*, 10(6):760–766, 2019.
- 693 C W Bacon and J F White. Stains, media, and procedures for analyzing endophytes. In *Biotech-*
694 *nology of endophytic fungi of grasses*, pages 47–56. CRC Press, 2018.
- 695 H Bakka, H Rue, G-A Fuglstad, A Riebler, D Bolin, J Illian, E Krainski, D Simpson, and F Lind-
696 gren. Spatial modeling with r-inla: A review. *Wiley Interdisciplinary Reviews: Computational*
697 *Statistics*, 10(6):e1443, 2018.
- 698 F T Bakker, V C Bieker, and M D Martin. Herbarium collection-based plant evolutionary genetics
699 and genomics. *Frontiers in Ecology and Evolution*, 8:603948, 2020.
- 700 D R Bazely, J P Ball, M Vicari, A J Tanentzap, M Bérenger, T Rakocevic, and S Koh. Broad-

- 701 scale geographic patterns in the distribution of vertically-transmitted, asexual endophytes in four
702 naturally-occurring grasses in sweden. *Ecography*, 30(3):367–374, 2007.
- 703 Sarah J Bearchell, Bart A Fraaije, Michael W Shaw, and Bruce DL Fitt. Wheat archive links long-
704 term fungal pathogen population dynamics to air pollution. *Proceedings of the National Academy
705 of Sciences*, 102(15):5438–5442, 2005.
- 706 J Beguin, S Martino, H Rue, and S G Cumming. Hierarchical analysis of spatially autocorrelated
707 ecological data using integrated nested laplace approximation. *Methods in Ecology and Evolution*,
708 3(5):921–929, 2012.
- 709 C S Berg, J L Brown, and J J Weber. An examination of climate-driven flowering-time shifts at
710 large spatial scales over 153 years in a common weedy annual. *American Journal of Botany*, 106
711 (11):1435–1443, 2019.
- 712 Christoph Bergmeir and José M Benítez. On the use of cross-validation for time series predictor
713 evaluation. *Information Sciences*, 191:192–213, 2012.
- 714 V C Bieker, F Sánchez Barreiro, J A Rasmussen, M Brunier, N Wales, and M D Martin. Metage-
715 nomic analysis of historical herbarium specimens reveals a postmortem microbial community.
716 *Molecular Ecology Resources*, 20(5):1206–1219, 2020.
- 717 J L Blois, P L Zarnetske, M C Fitzpatrick, and S Finnegan. Climate change and the past, present,
718 and future of biotic interactions. *Science*, 341(6145):499–504, 2013.
- 719 M Bradshaw, U Braun, M Elliott, J Kruse, S-Y Liu, G Guan, and P Tobin. A global genetic analysis
720 of herbarium specimens reveals the invasion dynamics of an introduced plant pathogen. *Fungal
721 Biology*, 125(8):585–595, 2021.
- 722 Michael J Bradshaw, Julie Carey, Miao Liu, Holly P Bartholomew, Wayne M Jurick, Sarah Hamble-
723 ton, Dylan Hendricks, Martin Schnittler, and Markus Scholler. Genetic time traveling: sequenc-
724 ing old herbarium specimens, including the oldest herbarium specimen sequenced from kingdom

- fungi, reveals the population structure of an agriculturally significant rust. *New Phytologist*, 237(4):1463–1473, 2023.
- D Brem and A Leuchtmann. *Epichloë* grass endophytes increase herbivore resistance in the woodland grass *Brachypodium sylvaticum*. *Oecologia*, 126(4):522–530, 2001.
- T A Carleton and S M Hsiang. Social and economic impacts of climate. *Science*, 353(6304):aad9837, 2016.
- S Cheng, Y-N Zou, K Kuča, A Hashem, E F Abd_Allah, and Q-S Wu. Elucidating the mechanisms underlying enhanced drought tolerance in plants mediated by arbuscular mycorrhizal fungi. *Frontiers in Microbiology*, 12:4029, 2021.
- K Clay and C Schardl. Evolutionary origins and ecological consequences of endophyte symbiosis with grasses. *The American Naturalist*, 160(S4):S99–S127, 2002.
- D G Clayton, L Bernardinelli, and C Montomoli. Spatial correlation in ecological analysis. *International Journal of Epidemiology*, 22(6):1193–1202, 1993.
- S D Côté, T P Rooney, J-P Tremblay, C Dussault, and D M Waller. Ecological impacts of deer overabundance. *Annu. Rev. Ecol. Evol. Syst.*, 35(1):113–147, 2004.
- KD Craven, PTW Hsiau, A Leuchtmann, W Hollin, and CL Schardl. Multigene phylogeny of *Epichloë* species, fungal symbionts of grasses. *Annals of the Missouri Botanical Garden*, pages 14–34, 2001.
- K M Crawford, J M Land, and J A Rudgers. Fungal endophytes of native grasses decrease insect herbivore preference and performance. *Oecologia*, 164:431–444, 2010.
- M S Crossley, T D Meehan, M D Moran, J Glassberg, W E Snyder, and A K Davis. Opposing global change drivers counterbalance trends in breeding North American monarch butterflies. *Global Change Biology*, 28(15):4726–4735, 2022.

- 748 C Daly and K Bryant. The PRISM climate and weather system — An introduction. *Corvallis, OR:*
749 *PRISM climate group*, 2, 2013.
- 750 B H Daru, D S Park, R B Primack, C G Willis, D S Barrington, T J S Whitfeld, T G Seidler, P W
751 Sweeney, D R Foster, A M Ellison, et al. Widespread sampling biases in herbaria revealed from
752 large-scale digitization. *New Phytologist*, 217(2):939–955, 2018.
- 753 B H Daru, E A Bowman, D H Pfister, and A E Arnold. A novel proof of concept for capturing
754 the diversity of endophytic fungi preserved in herbarium specimens. *Philosophical Transactions
755 of the Royal Society B*, 374(1763):20170395, 2019.
- 756 C C Davis, C G Willis, B Connolly, C Kelly, and A M Ellison. Herbarium records are reliable sources
757 of phenological change driven by climate and provide novel insights into species' phenological
758 cueing mechanisms. *American Journal of Botany*, 102(10):1599–1609, 2015.
- 759 Charles C Davis. The herbarium of the future. *Trends in Ecology & Evolution*, 38(5):412–423, 2023.
- 760 A J Davitt, M Stansberry, and H A Rudgers. Do the costs and benefits of fungal endophyte symbiosis
761 vary with light availability? *New Phytologist*, 188(3):824–834, 2010.
- 762 A J Davitt, C Chen, and J A Rudgers. Understanding context-dependency in plant–microbe sym-
763 biosis: The influence of abiotic and biotic contexts on host fitness and the rate of symbiont
764 transmission. *Environmental and Experimental Botany*, 71(2):137–145, 2011.
- 765 F A Decunta, L I Pérez, D P Malinowski, M A Molina-Montenegro, and P E Gundel. A systematic
766 review on the effects of *Epichloë* fungal endophytes on drought tolerance in cool-season grasses.
767 *Frontiers in Plant Science*, 12:644731, 2021.
- 768 M Di Luzio, G L Johnson, C Daly, J K Eischeid, and J G Arnold. Constructing retrospective
769 gridded daily precipitation and temperature datasets for the conterminous United States. *Journal
770 of Applied Meteorology and Climatology*, 47(2):475–497, 2008.

- 771 M L Donald, T F Bohner, K M Kolis, R A Shadow, J A Rudgers, and TEX Miller. Context-
772 dependent variability in the population prevalence and individual fitness effects of plant–fungal
773 symbiosis. *Journal of Ecology*, 109(2):847–859, 2021.
- 774 AE Douglas. Host benefit and the evolution of specialization in symbiosis. *Heredity*, 81(6):599–603,
775 1998.
- 776 Y-W Duan, H Ren, T Li, L-L Wang, Z-Q Zhang, Y-L Tu, and Y-P Yang. A century of pollination
777 success revealed by herbarium specimens of seed pods. *New Phytologist*, 224(4):1512–1517, 2019.
- 778 E J Edwards, B D Mishler, and C D Davis. University herbaria are uniquely important. *Trends in
779 Plant Science*.
- 780 M Engel, T Mette, and W Falk. Spatial species distribution models: Using Bayes inference with
781 INLA and SPDE to improve the tree species choice for important European tree species. *Forest
782 Ecology and Management*, 507:119983, 2022.
- 783 K D Erickson and A B Smith. Accounting for imperfect detection in data from museums and herbaria
784 when modeling species distributions: combining and contrasting data-level versus model-level bias
785 correction. *Ecography*, 44(9):1341–1352, 2021.
- 786 S M Evers, T M Knight, D W Inouye, TEX Miller, R Salguero-Gómez, A M Iler, and A Compagnoni.
787 Lagged and dormant season climate better predict plant vital rates than climate during the
788 growing season. *Global Change Biology*, 27(9):1927–1941, 2021.
- 789 P E M Fine. Vectors and vertical transmission: an epidemiologic perspective. *Annals of the New
790 York Academy of Sciences*, 266(1):173–194, 1975.
- 791 J C Fowler, M L Donald, J L Bronstein, and TEX Miller. The geographic footprint of mutualism:
792 How mutualists influence species’ range limits. *Ecological Monographs*, 93(1):e1558, 2023.
- 793 J C Fowler, S Ziegler, K D Whitney, J A Rudgers, and TEX Miller. Microbial symbionts buffer

- 794 hosts from the demographic costs of environmental stochasticity. *Ecology Letters*, 27(5):e14438,
795 2024.
- 796 PR Fraude, F De Jongh, F Vermeulen, J Van Bleijswijk, and RPM Bak. Variation in symbiont
797 distribution between closely related coral species over large depth ranges. *Molecular Ecology*, 17
798 (2):691–703, 2008.
- 799 M E Frederickson. Mutualisms are not on the verge of breakdown. *Trends in Ecology & Evolution*,
800 32(10):727–734, 2017.
- 801 W Gaul, D Sadykova, H J White, L Leon-Sanchez, P Caplat, M C Emmerson, and J M Yearsley.
802 Data quantity is more important than its spatial bias for predictive species distribution modelling.
803 *PeerJ*, 8:e10411, 2020.
- 804 GBIF.Org. Occurrence download, 2025a. URL <https://www.gbif.org/occurrence/download/>
805 0018831-250127130748423.
- 806 GBIF.Org. Occurrence download, 2025b. URL <https://www.gbif.org/occurrence/download/>
807 0018850-250127130748423.
- 808 GBIF.Org. Occurrence download, 2025c. URL <https://www.gbif.org/occurrence/download/>
809 0018851-250127130748423.
- 810 A Gelman and J Hill. *Data analysis using regression and multilevel/hierarchical models*. Cambridge
811 University Press, 2006.
- 812 S E Gilman, M C Urban, J Tewksbury, G W Gilchrist, and R D Holt. A framework for community
813 interactions under climate change. *Trends in Ecology & Evolution*, 25(6):325–331, 2010.
- 814 G Granath, M Vicari, D R Bazely, J P Ball, A Puentes, and T Rakocevic. Variation in the abundance
815 of fungal endophytes in fescue grasses along altitudinal and grazing gradients. *Ecography*, 30(3):
816 422–430, 2007.

- 817 A Gross, C Petitcollin, C Dutech, B Ly, M Massot, J Faivre d'Arcier, L Dubois, G Saint-Jean, and
818 M-L Desprez-Loustau. Hidden invasion and niche contraction revealed by herbaria specimens
819 in the fungal complex causing oak powdery mildew in europe. *Biological Invasions*, 23:885–901,
820 2021.
- 821 P E Gundel, I Zabalgogeazcoa, and BRV De Aldana. Interaction between plant genotype and
822 the symbiosis with *Epichloë* fungal endophytes in seeds of red fescue (*Festuca rubra*). *Crop and*
823 *Pasture Science*, 62(11):1010–1016, 2011.
- 824 P E Gundel, A C Ueno, C Casas, TEX Miller, L I Pérez, R Cuyeu, and M Omacini. Temporal
825 host–symbiont dynamics in community contexts: Impacts of host fitness and vertical transmission
826 efficiency on symbiosis prevalence. *Functional Ecology*, 38(12):2610–2622, 2024.
- 827 E K Hart and K Bell. *prism: Download data from the Oregon prism project*, 2015. URL <https://github.com/ropensci/prism>. R package version 0.0.6.
- 828
- 829 J J Heberling and D J Burke. Utilizing herbarium specimens to quantify historical mycorrhizal
830 communities. *Applications in plant sciences*, 7(4):e01223, 2019.
- 831 R J Hijmans, S Phillips, J Leathwick, J Elith, and Robert J Hijmans. Package ‘dismo’. *Circles*, 9
832 (1):1–68, 2017.
- 833 J HilleRisLambers, M A Harsch, A K Ettinger, K R Ford, and E J Theobald. How will biotic
834 interactions influence climate change-induced range shifts? *Annals of the New York Academy of*
835 *Sciences*, 1297(1):112–125, 2013.
- 836 IPCC. Climate change 2021: The physical science basis, 2021. URL <https://www.ipcc.ch/report/ar6/wg1/>.
- 837
- 838 N J B Isaac, M A Jarzyna, P Keil, L I Dambly, P H Boersch-Supan, E Browning, S N Freeman,
839 N Golding, G Guillera-Arroita, P A Henrys, et al. Data integration for large-scale models of
840 species distributions. *Trends in Ecology & Evolution*, 35(1):56–67, 2020.

- 841 Gareth James, Daniela Witten, Trevor Hastie, Robert Tibshirani, et al. *An introduction to statistical*
842 *learning*, volume 112. Springer, 2013.
- 843 A Jiménez-Valverde. Insights into the area under the receiver operating characteristic curve (auc)
844 as a discrimination measure in species distribution modelling. *Global Ecology and Biogeography*,
845 21(4):498–507, 2012.
- 846 D Kahle and H Wickham. Package ‘ggmap’. *Retrieved September*, 5:2021, 2019.
- 847 M R Kazenel, C L Debban, L Ranelli, W Q Hendricks, Y A Chung, T H Pendergast IV, N D
848 Charlton, C A Young, and J A Rudgers. A mutualistic endophyte alters the niche dimensions of
849 its host plant. *AoB plants*, 7:plv005, 2015.
- 850 R A Knapp, G M Fellers, P M Kleeman, D AW Miller, V T Vredenburg, E B Rosenblum, and C J
851 Briggs. Large-scale recovery of an endangered amphibian despite ongoing exposure to multiple
852 stressors. *Proceedings of the National Academy of Sciences*, 113(42):11889–11894, 2016.
- 853 M V Kozlov, I V Sokolova, V Zverev, A A Egorov, M Y Goncharov, and E L Zvereva. Biases in
854 estimation of insect herbivory from herbarium specimens. *Scientific Reports*, 10(1):12298, 2020.
- 855 Marcus Lapeyrolerie and Carl Boettiger. Limits to ecological forecasting: Estimating uncertainty
856 for critical transitions with deep learning. *Methods in Ecology and Evolution*, 14(3):785–798, 2023.
- 857 B R Lee, E F Alecrim, T K Miller, J RK Forrest, J M Heberling, R B Primack, and R D Sargent.
858 Phenological mismatch between trees and wildflowers: Reconciling divergent findings in two recent
859 analyses. *Journal of Ecology*, 112(6):1184–1199, 2024.
- 860 J Lendemer, B Thiers, A K Monfils, J Zaspel, E R Ellwood, A Bentley, K LeVan, J Bates, D Jen-
861 nings, D Contreras, et al. The extended specimen network: A strategy to enhance us biodiversity
862 collections, promote research and education. *BioScience*, 70(1):23–30, 2020.
- 863 A Leuchtmann. Systematics, distribution, and host specificity of grass endophytes. *Natural Toxins*,
864 1(3):150–162, 1992.

- 865 A Leuchtmann, C W Bacon, C L Schardl, J F White Jr, and M Tadych. Nomenclatural realignment
866 of *Neotyphodium* species with genus *Epichloë*. *Mycologia*, 106(2):202–215, 2014.
- 867 F Lindgren, H Rue, and J Lindström. An explicit link between gaussian fields and gaussian markov
868 random fields: the stochastic partial differential equation approach. *Journal of the Royal Statis-*
869 *tical Society: Series B (Statistical Methodology)*, 73(4):423–498, 2011.
- 870 C Liu, P M Berry, T P Dawson, and R G Pearson. Selecting thresholds of occurrence in the
871 prediction of species distributions. *Ecography*, 28(3):385–393, 2005.
- 872 D D Mc Cargo, L J Iannone, M V Vignale, C L Schardl, and M S Rossi. Species diversity of
873 *Epichloë* symbiotic with two grasses from southern Argentinean Patagonia. *Mycologia*, 106(2):
874 339–352, 2014.
- 875 M McFall-Ngai, M G Hadfield, TCG Bosch, H V Carey, T Domazet-Lošo, A E Douglas, N Dubilier,
876 G Eberl, T Fukami, S F Gilbert, et al. Animals in a bacterial world, a new imperative for the
877 life sciences. *Proceedings of the National Academy of Sciences*, 110(9):3229–3236, 2013.
- 878 T D Meehan, N L Michel, and H Rue. Spatial modeling of Audubon Christmas Bird Counts reveals
879 fine-scale patterns and drivers of relative abundance trends. *Ecosphere*, 10(4):e02707, 2019.
- 880 E K Meineke and B H Daru. Bias assessments to expand research harnessing biological collections.
881 *Trends in Ecology & Evolution*, 36(12):1071–1082, 2021.
- 882 E K Meineke, C C Davis, and T J Davies. The unrealized potential of herbaria for global change
883 biology. *Ecological Monographs*, 88(4):505–525, 2018.
- 884 E K Meineke, A T Classen, N J Sanders, and T J Davies. Herbarium specimens reveal increasing
885 herbivory over the past century. *Journal of Ecology*, 107(1):105–117, 2019.
- 886 A R Meyer, M Valentin, L Liulevicius, T R McDonald, M P Nelsen, J Pengra, R J Smith, and
887 D Stanton. Climate warming causes photobiont degradation and c starvation in a boreal climate
888 sentinel lichen. *American Journal of Botany*, 2022.

- 889 D AW Miller, K Pacifici, J S Sanderlin, and B J Reich. The recent past and promising future for
890 data integration methods to estimate species' distributions. *Methods in Ecology and Evolution*,
891 10(1):22–37, 2019.
- 892 D S Park, I Breckheimer, A C Williams, E Law, A M Ellison, and C C Davis. Herbarium specimens
893 reveal substantial and unexpected variation in phenological sensitivity across the eastern United
894 States. *Philosophical Transactions of the Royal Society B*, 374(1763):20170394, 2019.
- 895 B J Parker, J Hrček, AHC McLean, and H C J Godfray. Genotype specificity among hosts,
896 pathogens, and beneficial microbes influences the strength of symbiont-mediated protection. *Evo-
897 lution*, 71(5):1222–1231, 2017.
- 898 M Parniske. Arbuscular mycorrhiza: The mother of plant root endosymbioses. *Nature Reviews
899 Microbiology*, 6(10):763–775, 2008.
- 900 A Pauw and J A Hawkins. Reconstruction of historical pollination rates reveals linked declines of
901 pollinators and plants. *Oikos*, 120(3):344–349, 2011.
- 902 S Piao, Q Liu, A Chen, I A Janssens, Y Fu, J Dai, L Liu, X Lian, M Shen, and X Zhu. Plant
903 phenology and global climate change: Current progresses and challenges. *Global Change Biology*,
904 25(6):1922–1940, 2019.
- 905 T Poisot, G Bergeron, K Cazelles, T Dallas, D Gravel, A MacDonald, B Mercier, C Violet, and
906 S Vissault. Global knowledge gaps in species interaction networks data. *Journal of Biogeography*,
907 48(7):1552–1563, 2021.
- 908 N E Rafferty, P J CaraDonna, and J L Bronstein. Phenological shifts and the fate of mutualisms.
909 *Oikos*, 124(1):14–21, 2015.
- 910 Emma Chollet Ramampiandra, Andreas Scheidegger, Jonas Wydler, and Nele Schuwirth. A com-
911 parison of machine learning and statistical species distribution models: Quantifying overfitting
912 supports model interpretation. *Ecological Modelling*, 481:110353, 2023.

- 913 C J Raxworthy and B T Smith. Mining museums for historical DNA: Advances and challenges in
914 museomics. *Trends in Ecology & Evolution*, 36(11):1049–1060, 2021.
- 915 F Renoz, I Pons, and T Hance. Evolutionary responses of mutualistic insect–bacterial symbioses in
916 a world of fluctuating temperatures. *Current Opinion in Insect Science*, 35:20–26, 2019.
- 917 Jean B Ristaino. The importance of mycological and plant herbaria in tracking plant killers. *Fron-
918 tiers in Ecology and Evolution*, 7:521, 2020.
- 919 Jean B Ristaino, Carol T Groves, and Gregory R Parra. Pcr amplification of the irish potato famine
920 pathogen from historic specimens. *Nature*, 411(6838):695–697, 2001.
- 921 Jean Beagle Ristaino. Tracking historic migrations of the irish potato famine pathogen, phytoph-
922 thora infestans. *Microbes and infection*, 4(13):1369–1377, 2002.
- 923 E L Roberts and A Ferraro. Rhizosphere microbiome selection by *Epichloë* endophytes of *Festuca*
924 *arundinacea*. *Plant and Soil*, 396:229–239, 2015.
- 925 RJ Rodriguez, JF White Jr, Anne E Arnold, and a RS and Redman. Fungal endophytes: diversity
926 and functional roles. *New Phytologist*, 182(2):314–330, 2009.
- 927 G Rolshausen, F Dal Grande, A D Sadowska-Deś, J Otte, and I Schmitt. Quantifying the climatic
928 niche of symbiont partners in a lichen symbiosis indicates mutualist-mediated niche expansions.
929 *Ecography*, 41(8):1380–1392, 2018.
- 930 J A Rudgers, M E Afkhami, M A Rúa, A J Davitt, S Hammer, and V M Huguet. A fungus among
931 us: broad patterns of endophyte distribution in the grasses. *Ecology*, 90(6):1531–1539, 2009.
- 932 J A Rudgers, M E Afkhami, L Bell-Dereske, Y A Chung, K M Crawford, S N Kivlin, M A Mann,
933 and M A Nuñez. Climate disruption of plant-microbe interactions. *Annual review of ecology,
934 evolution, and systematics*, 51(1):561–586, 2020.
- 935 Jennifer A Rudgers and Angela L Swafford. Benefits of a fungal endophyte in *Elymus virginicus*
936 decline under drought stress. *Basic and Applied Ecology*, 10(1):43–51, 2009.

- 937 H Rue, S Martino, and N Chopin. Approximate bayesian inference for latent gaussian models by
938 using integrated nested laplace approximations. *Journal of the royal statistical society: Series b*
939 (*statistical methodology*), 71(2):319–392, 2009.
- 940 R F Sage. Global change biology: a primer. *Global Change Biology*, 26(1):3–30, 2020.
- 941 K Saikkonen, P E Gundel, and M Helander. Chemical ecology mediated by fungal endophytes in
942 grasses. *Journal of chemical ecology*, 39:962–968, 2013.
- 943 C L Schardl, C A Young, J R Faulkner, S Florea, and J Pan. Chemotypic diversity of *Epichloae*,
944 fungal symbionts of grasses. *Fungal Ecology*, 5(3):331–344, 2012.
- 945 Ryan J Schmidt, Kristen E Saban, Lena Struwe, and Charles C Davis. The collector practices that
946 shape spatial, temporal, and taxonomic bias in herbaria. *New Phytologist*.
- 947 María Semmartin, Marina Omacini, Pedro E Gundel, and Ignacio M Hernández-Agramonte. Broad-
948 scale variation of fungal-endophyte incidence in temperate grasses. *Journal of Ecology*, 103(1):
949 184–190, 2015.
- 950 S I Seneviratne, X Zhang, M Adnan, W Badi, C Dereczynski, A D Luca, S Ghosh, I Iskandar,
951 J Kossin, S Lewis, et al. Weather and climate extreme events in a changing climate. 2021.
- 952 D Simpson, H Rue, A Riebler, T G Martins, and S H Sørbye. Penalising model component com-
953 plexity: A principled, practical approach to constructing priors. 2017.
- 954 Brajesh K Singh, Manuel Delgado-Baquerizo, Eleonora Egidi, Emilio Guirado, Jan E Leach, Hong-
955 wei Liu, and Pankaj Trivedi. Climate change impacts on plant pathogens, food security and paths
956 forward. *Nature Reviews Microbiology*, 21(10):640–656, 2023.
- 957 Michelle E Sneck, Jennifer A Rudgers, Carolyn A Young, and Tom EX Miller. Variation in the
958 prevalence and transmission of heritable symbionts across host populations in heterogeneous en-
959 vironments. *Microbial Ecology*, 74:640–653, 2017.

- 960 Pamela S Soltis. Digitization of herbaria enables novel research. *American journal of botany*, 104
961 (9):1281–1284, 2017.
- 962 T F Stocker, D Qin, G-K Plattner, L V Alexander, S K Allen, N L Bindoff, F-M Bréon, J A Church,
963 U Cubasch, S Emori, et al. Technical summary. In *Climate Change 2013: The Physical Science
964 Basis. Contribution of Working Group I to the Fifth Assessment Report of the Intergovernmental
965 Panel on Climate Change*, pages 33–115. Cambridge University Press, 2013.
- 966 P A Stott, N P Gillett, G C Hegerl, D J Karoly, D A Stone, X Zhang, and F Zwiers. Detection and
967 attribution of climate change: A regional perspective. *Wiley Interdisciplinary Reviews: Climate
968 Change*, 1(2):192–211, 2010.
- 969 S Sully, DE Burkepile, MK Donovan, G Hodgson, and R Van Woesik. A global analysis of coral
970 bleaching over the past two decades. *Nature communications*, 10(1):1–5, 2019.
- 971 E Toby Kiers, T M Palmer, A R Ives, J F Bruno, and J L Bronstein. Mutualisms in a changing
972 world: an evolutionary perspective. *Ecology Letters*, 13(12):1459–1474, 2010.
- 973 A T Tredennick, G Hooker, S P Ellner, and P B Adler. A practical guide to selecting models for
974 exploration, inference, and prediction in ecology. *Ecology*, 102(6):e03336, 2021.
- 975 A D Treindl, J Stapley, and A Leuchtmann. Genetic diversity and population structure of *Epichloë*
976 fungal pathogens of plants in natural ecosystems. *Frontiers in Ecology and Evolution*, 11:1129867,
977 2023.
- 978 K E Trenberth, J T Fasullo, and T G Shepherd. Attribution of climate extreme events. *Nature
979 Climate Change*, 5(8):725–730, 2015.
- 980 A M Truitt, M Kapun, R Kaur, and W J Miller. Wolbachia modifies thermal preference in drosophila
981 melanogaster. *Environmental microbiology*, 21(9):3259–3268, 2019.
- 982 Shripad D. Tuljapurkar. Population dynamics in variable environments. III. Evolutionary dynamics
983 of r-selection. *Theoretical Population Biology*, 21(1):141–165, February 1982. ISSN 0040-5809.

- 984 doi: 10.1016/0040-5809(82)90010-7. URL <http://www.sciencedirect.com/science/article/pii/0040580982900107>.
- 985
- 986 A Urdangarin, T Goicoa, and M D Ugarte. Evaluating recent methods to overcome spatial con-
987 founding. *Revista Matemática Complutense*, 36(2):333–360, 2023.
- 988 V Vikuk, C A Young, S T Lee, P Nagabhyru, M Krischke, M J Mueller, and J Krauss. Infection
989 rates and alkaloid patterns of different grass species with systemic *Epichloë* endophytes. *Applied*
990 *and Environmental Microbiology*, 85(17):e00465–19, 2019.
- 991 M von Cräutlein, M Helander, H Korpelainen, P H Leinonen, B R Vázquez de Aldana, C A Young,
992 I Zabalgojgeazcoa, and K Saikkonen. Genetic diversity of the symbiotic fungus *Epichloë festucae*
993 in naturally occurring host grass populations. *Frontiers in Microbiology*, 12:756991, 2021.
- 994 Z Wang, C Li, and J White. Effects of *Epichloë* endophyte infection on growth, physiological
995 properties and seed germination of wild barley under saline conditions. *Journal of Agronomy and*
996 *Crop Science*, 206(1):43–51, 2020.
- 997 Eric J Ward, Eli E Holmes, James T Thorson, and Ben Collen. Complexity is costly: a meta-
998 analysis of parametric and non-parametric methods for short-term population forecasting. *Oikos*,
999 123(6):652–661, 2014.
- 1000 R J Warren and M A Bradford. Mutualism fails when climate response differs between interacting
1001 species. *Global Change Biology*, 20(2):466–474, 2014.
- 1002 N S Webster, R E Cobb, and A P Negri. Temperature thresholds for bacterial symbiosis with a
1003 sponge. *The ISME journal*, 2(8):830–842, 2008.
- 1004 J F White and G T Cole. Endophyte-host associations in forage grasses. i. Distribution of fungal
1005 endophytes in some species of *Lolium* and *Festuca*. *Mycologia*, 77(2):323–327, 1985.
- 1006 F M Willems, JF Scheepens, and O Bossdorf. Forest wildflowers bloom earlier as europe warms:
1007 Lessons from herbaria and spatial modelling. *New Phytologist*, 235(1):52–65, 2022.

- 1008 C G Willis, E R Ellwood, R B Primack, C C Davis, K D Pearson, A S Gallinat, J M Yost, G Nelson,
1009 S J Mazer, N L Rossington, et al. Old plants, new tricks: Phenological research using herbarium
1010 specimens. *Trends in Ecology & Evolution*, 32(7):531–546, 2017.
- 1011 C Xia, N Li, Y Zhang, C Li, X Zhang, and Z Nan. Role of *Epichloë* endophytes in defense responses
1012 of cool-season grasses to pathogens: A review. *Plant Disease*, 102(11):2061–2073, 2018.
- 1013 K Yoshida, E Sasaki, and S Kamoun. Computational analyses of ancient pathogen DNA from
1014 herbarium samples: Challenges and prospects. *Frontiers in Plant Science*, 6:771, 2015.
- 1015 Kentaro Yoshida, Verena J Schuenemann, Liliana M Cano, Marina Pais, Bagdevi Mishra, Rahul
1016 Sharma, Chirsta Lanz, Frank N Martin, Sophien Kamoun, Johannes Krause, et al. The rise and
1017 fall of the *Phytophthora infestans* lineage that triggered the irish potato famine. *elife*, 2:e00731,
1018 2013.

1019

Appendix A

1020

1021 *Appendix to "Increasing Prevalence of plant-fungal symbiosis across two*
1022 *centuries of environmental change"*

1023 **Authors:**

1024 Joshua C. Fowler^{1,2*}

1025 Jacob Moutouama¹

1026 Tom E. X. Miller¹

1027

1028 1. Rice University, Department of BioSciences, Houston, Texas 77006

1029 2. University of Miami, Department of Biology, Miami, Florida

1030 * Corresponding author; e-mail: jcf221@miami.edu.

1031 **Contents:**

1032 Appendix A includes: Figure A1 - Figure A15, Table A1, and Supporting Methods).

1033

Supplemental Figures

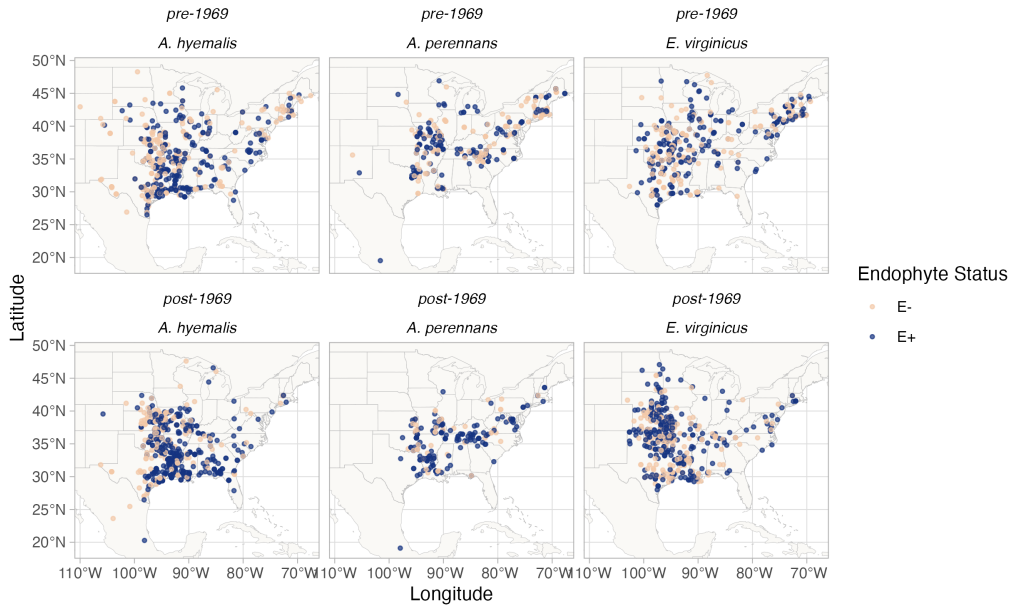


Figure A1: **Endophyte presence/absence in specimens of each host species.** Points show collection locations colored according to whether the specimen contained endophytes (E+; blue points) or did not contain endophytes (E-, tan points). To visualize temporal change, the data are faceted before and after the median year of collection. Map lines delineate study areas and do not necessarily depict accepted national boundaries.

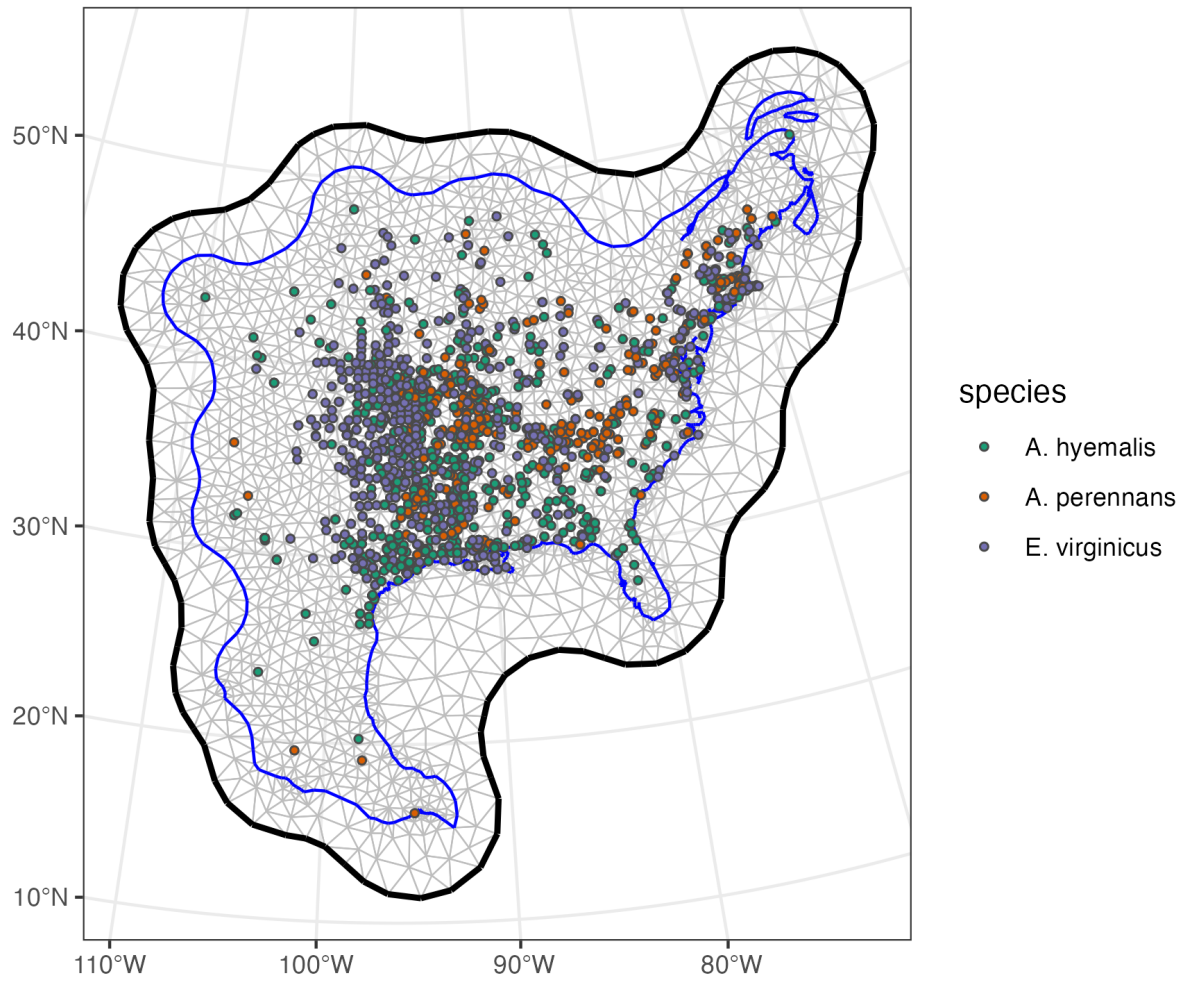


Figure A2: **Triangulation mesh used to estimate spatial dependence between data points.**

Grey lines indicate edges of triangles used to define distances between observations. Colored points indicate locations of sampled herbarium specimens for each host species, and the blue line shows the convex hull and coastline used to define the edge of the mesh around the data points. The thick black line shows the convex hull defining a buffer space around the edge of the mesh to reduce the influence of edge effects on model estimates.

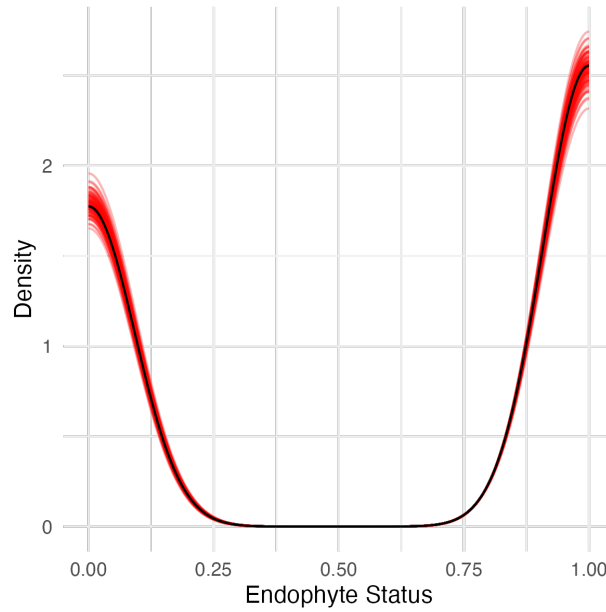


Figure A3: **Graphical posterior predictive check of the endophyte prevalence model fit.**

Consistency between observed data and predicted values indicate that the fitted model accurately describes the data. Graph shows density curves for the observed data (black) along with 100 predicted datasets (red).

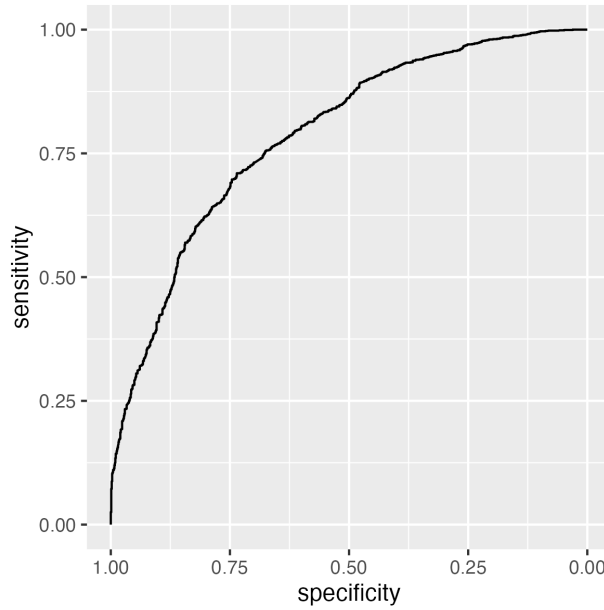


Figure A4: ROC plot showing performance of the endophyte prevalence model in classifying observations according to endophyte status within the in-sample training data from herbarium collections. The curves show adequate model performance for observed data. The AUC value is 0.79.

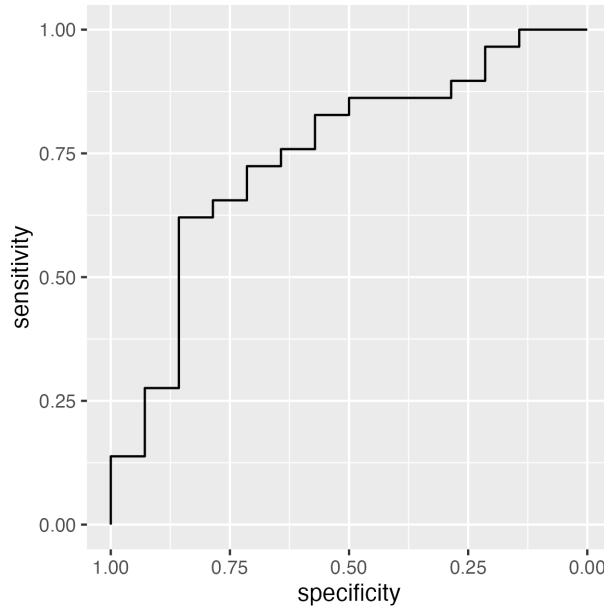


Figure A5: ROC plot showing performance of the endophyte prevalence model in classifying observations according to endophyte status within the out-of-sample test data from contemporary surveys. The curves show adequate model performance for test data. The AUC value is 0.77.

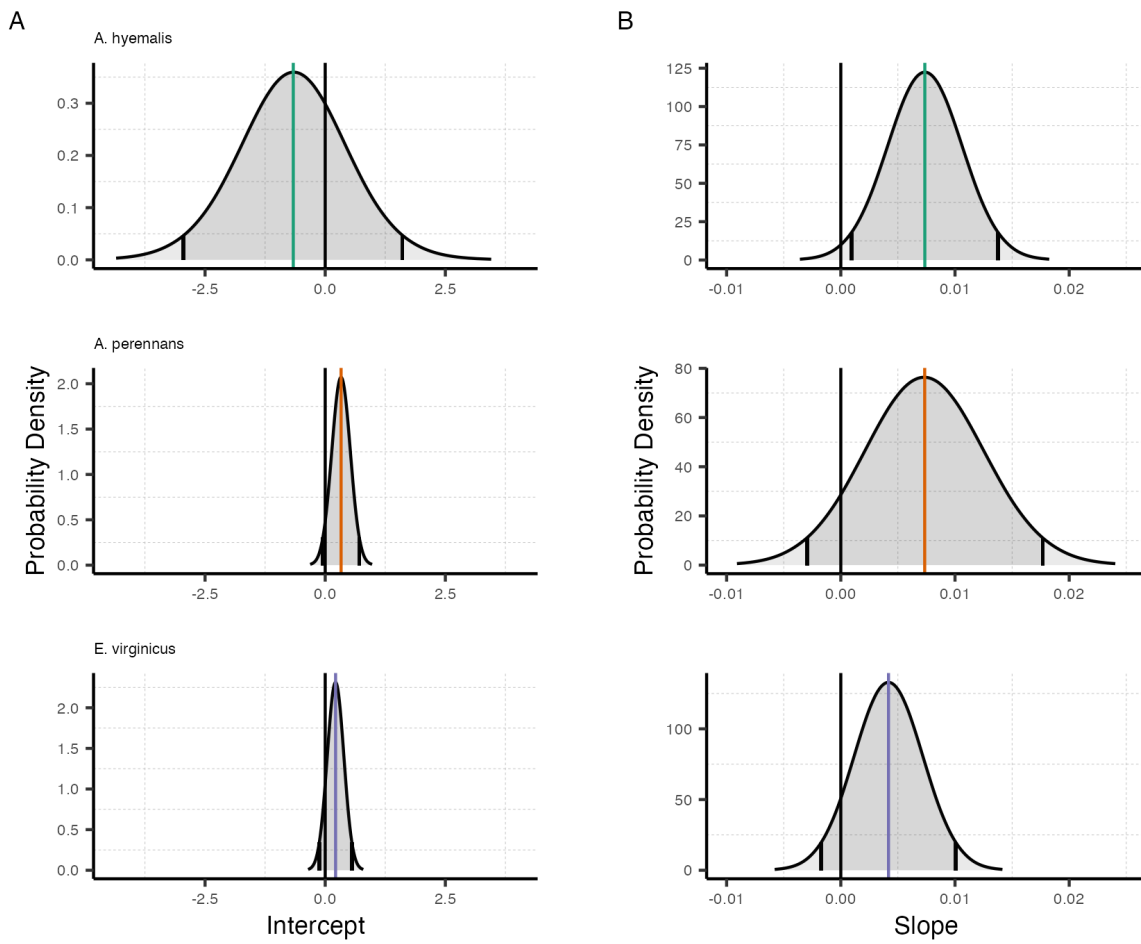


Figure A6: Posterior estimates of parameters describing global intercept and temporal trends from the endophyte prevalence model. Density curves show the probability density along with mean (colored line) and 95% CI (black lines) for the (A) intercept and (B) slope terms, A and T respectively from Eqn. 1. Colors represent each host species

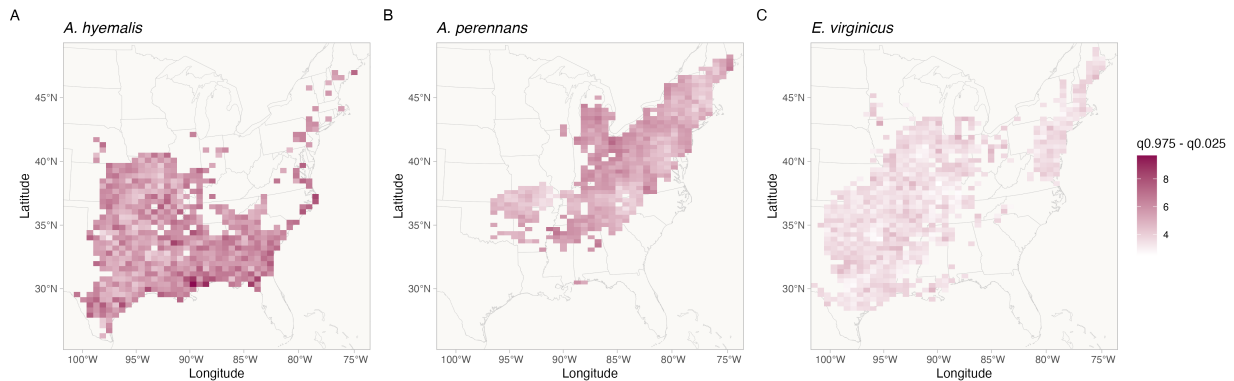


Figure A7: Credible interval width of temporal trends in endophyte prevalence across the distribution of each host species estimated from the endophyte prevalence model.
 Shading represents the range of the 95% posterior credible interval given in units of *% change in prevalence/year* for spatially varying slopes, τ from Eqn. 1. Map lines delineate study areas and do not necessarily depict accepted national boundaries.

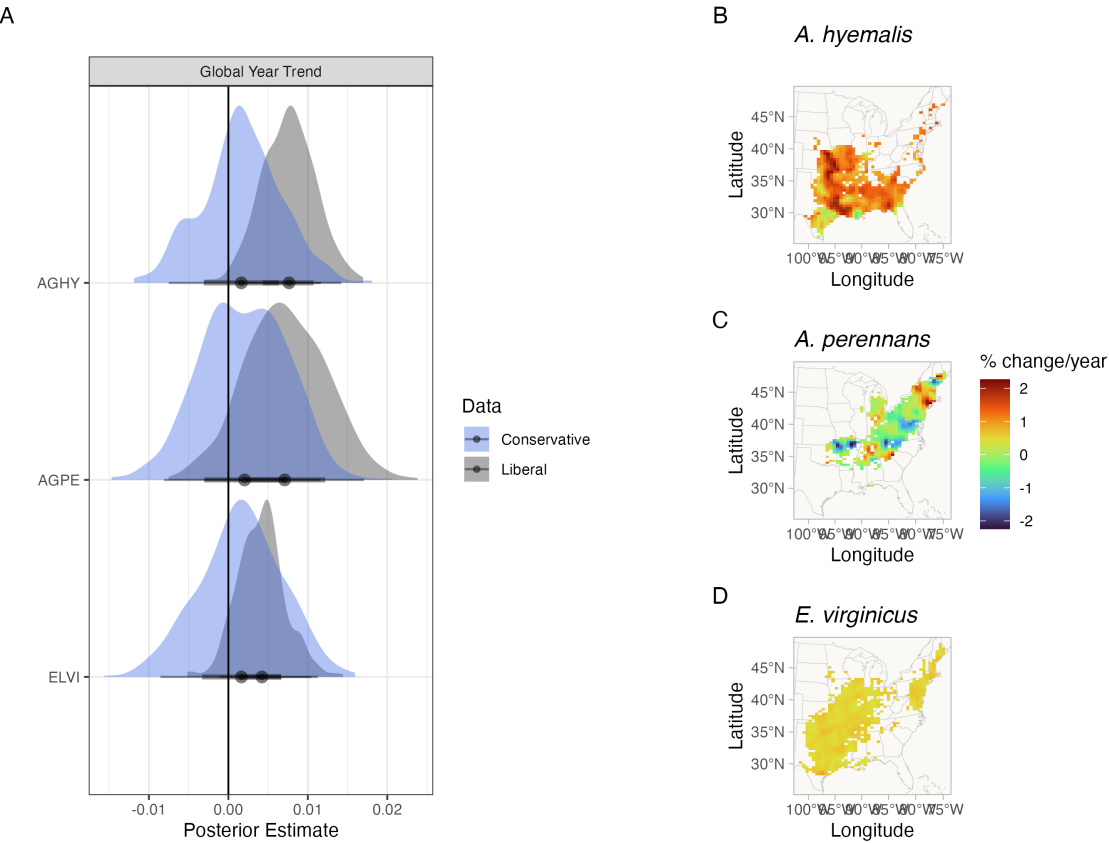


Figure A8: Comparison of endophyte prevalence model estimates fit to data with liberal versus conservative endophyte scores. Liberal and conservative scores document uncertainty in the endophyte identification process. Each specimen was given both a liberal and conservative scores. In cases of uncertain identification, the liberal status assumed a potential endophyte identification was more likely to be endophyte-positive while the conservative status assumed that the potential endophyte identification was less likely to be endophyte-positive. (A) Posterior estimates of global temporal trend (T from Eqn. 1) for the endophyte prevalence model fit to liberal scores (grey) and to conservative scores (blue). Maps show the spatially varying temporal trend estimates (τ from Eqn. 1) from the endophyte prevalence model fit to conservative scores for (B) *A. hyemalis*, (C) *A. perennans*, and (D) *E. virginicus*. Note that the color scale differs between this visualization and Fig. 3 that shows estimates fit using liberal endophyte scores.

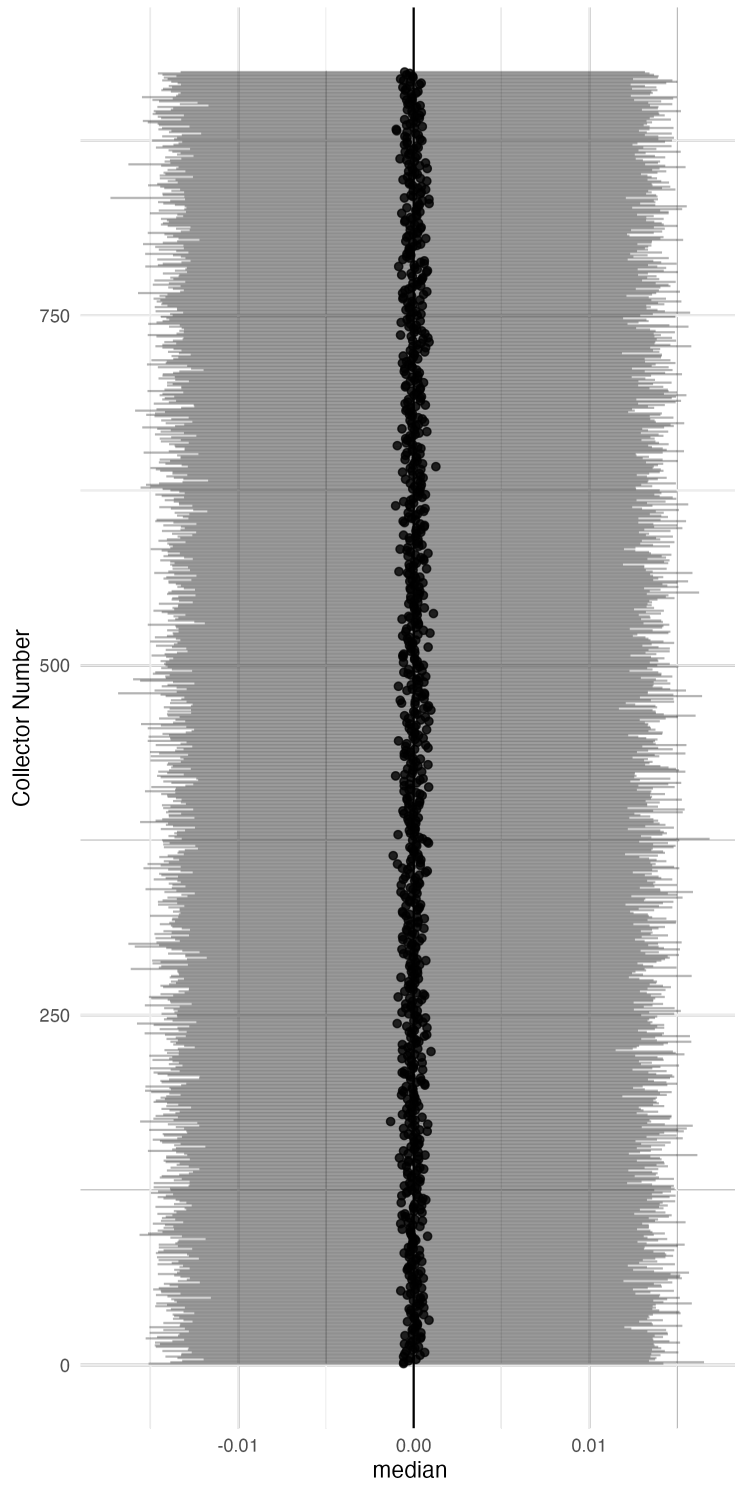


Figure A9: **Posterior estimates of collector random effects from endophyte prevalence model.** Collector random effects are denoted χ in Eqn. 1 and represent variance associated with researchers who collected historic herbarium specimens. Points show posterior median along with 95% CI for each of 924 individual collectors.

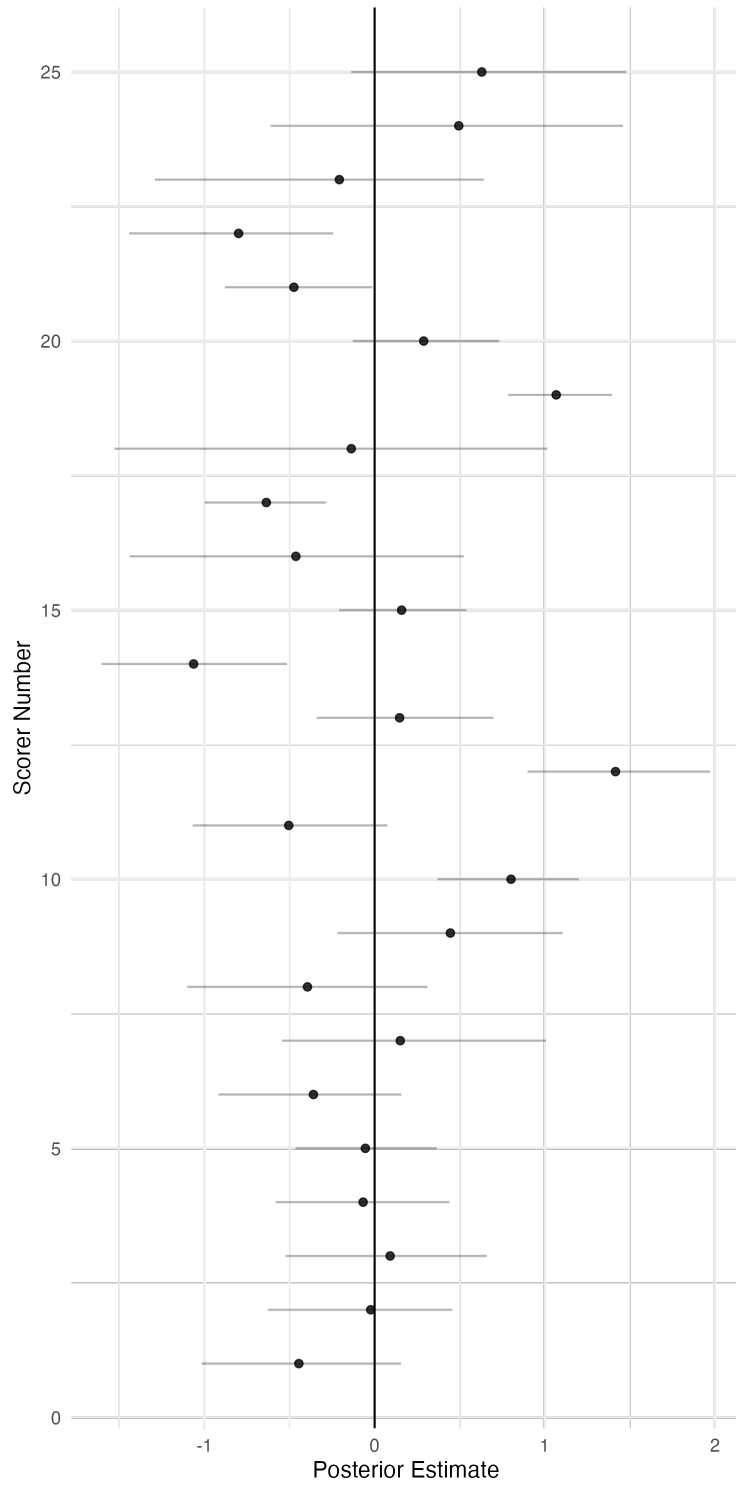


Figure A10: Posterior estimates of scorer random effects from endophyte prevalence model. Scorer random effects are denoted ω in Eqn. 1 and represent variance associated with researchers who identified *Epichloë* endophytes within herbarium specimen tissue samples. Points show posterior median along with 95% CI for each of 25 individual scorers.

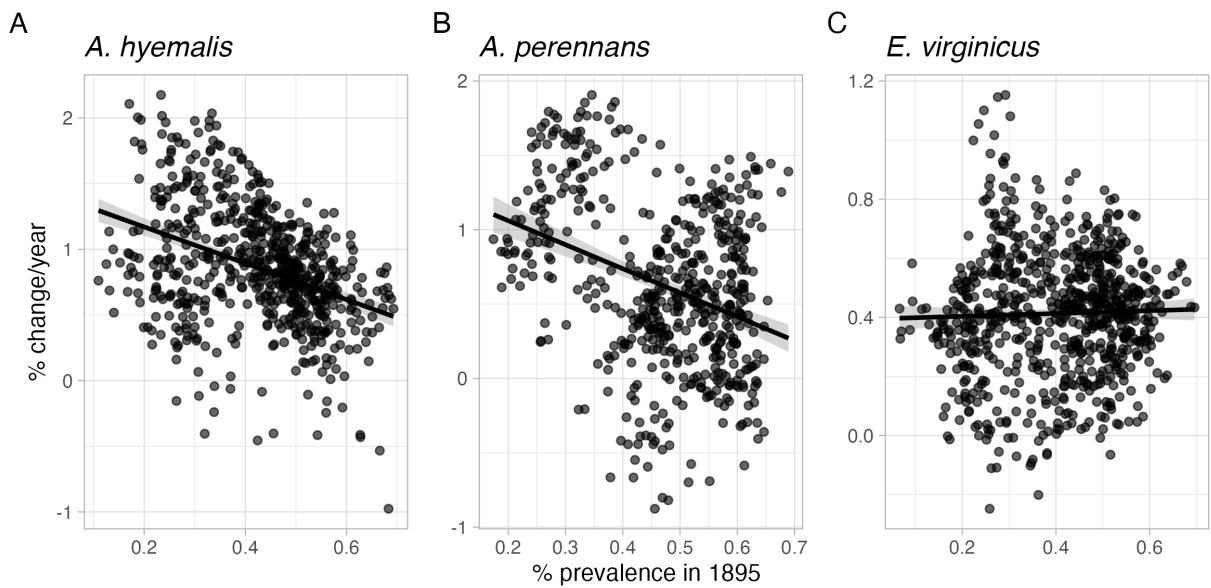


Figure A11: Relationship between initial prevalence and temporal trends in prevalence estimated from the endophyte prevalence model. Points show predicted posterior mean temporal trend for each species at pixels across each host distribution ((A) *A. hyemalis*, (B) *A. perennans*, and (C) *E. virginicus*). along with a linear regression and shaded ribbon showing 95% confidence interval.

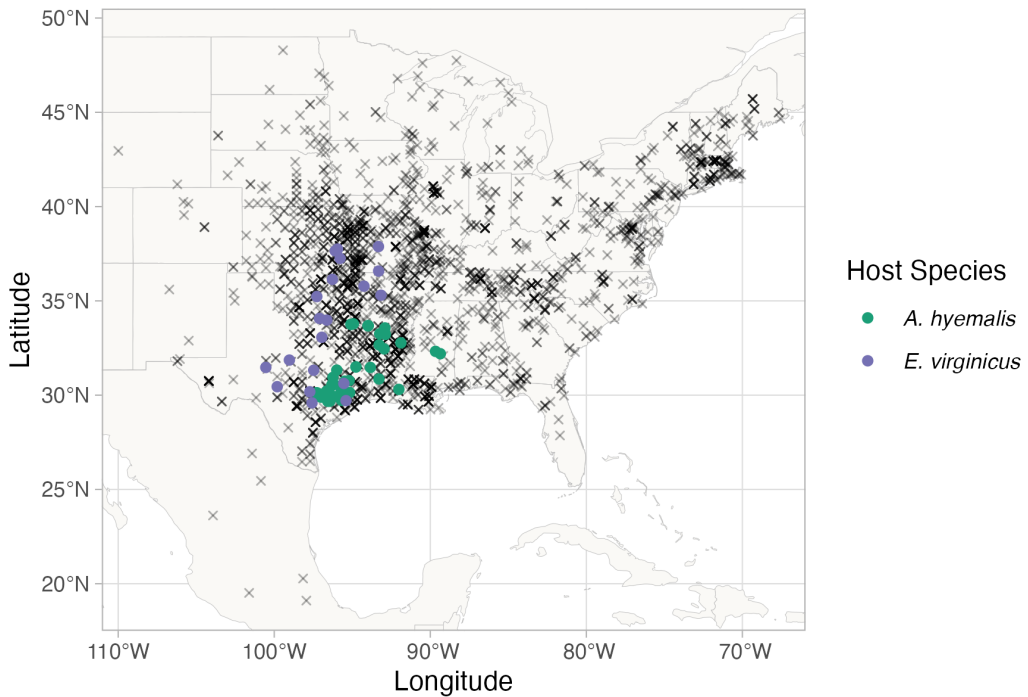


Figure A12: Locations of contemporary surveys of endophytes used as "test" data to evaluate predictive ability of the endophyte prevalence model. Points are locations of host populations surveyed between 2013 and 2019 for endophytes, colored by species (*A. hyemalis*: green, *E. virginicus*: purple). Black crosses show the historical herbarium collection locations used as "training" data for the endophyte prevalence model.

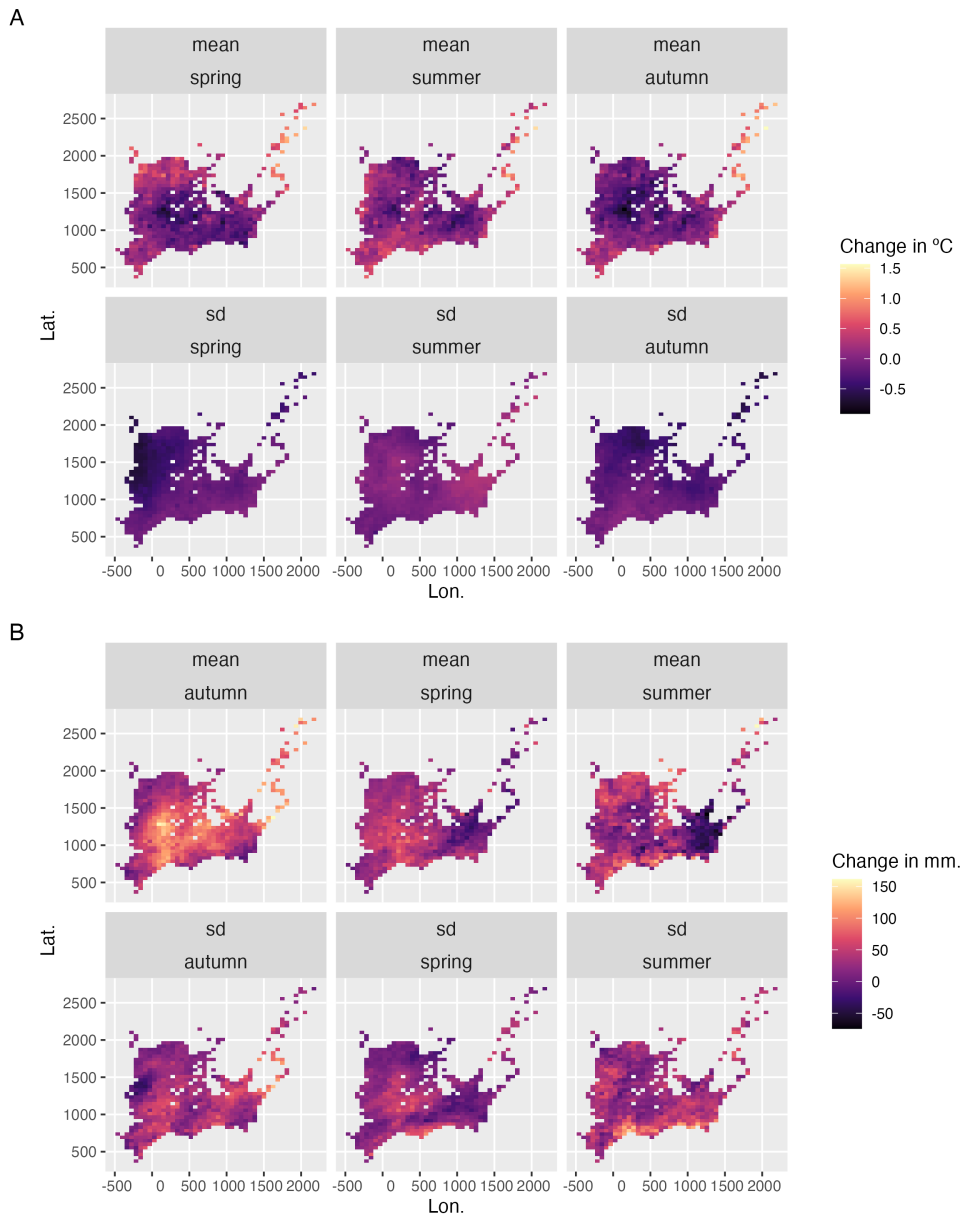


Figure A13: **Change in seasonal climate variables between the periods 1895-1925 and 1990-2020 across the distribution of *A. hyemalis*.** Color represents change in (A) seasonal temperature ($^{\circ}\text{C}$) and (B) seasonal precipitation (mm.). Maps show pixels covering the modeled distribution of *A. hyemalis* used in *post hoc* climate regression analysis.

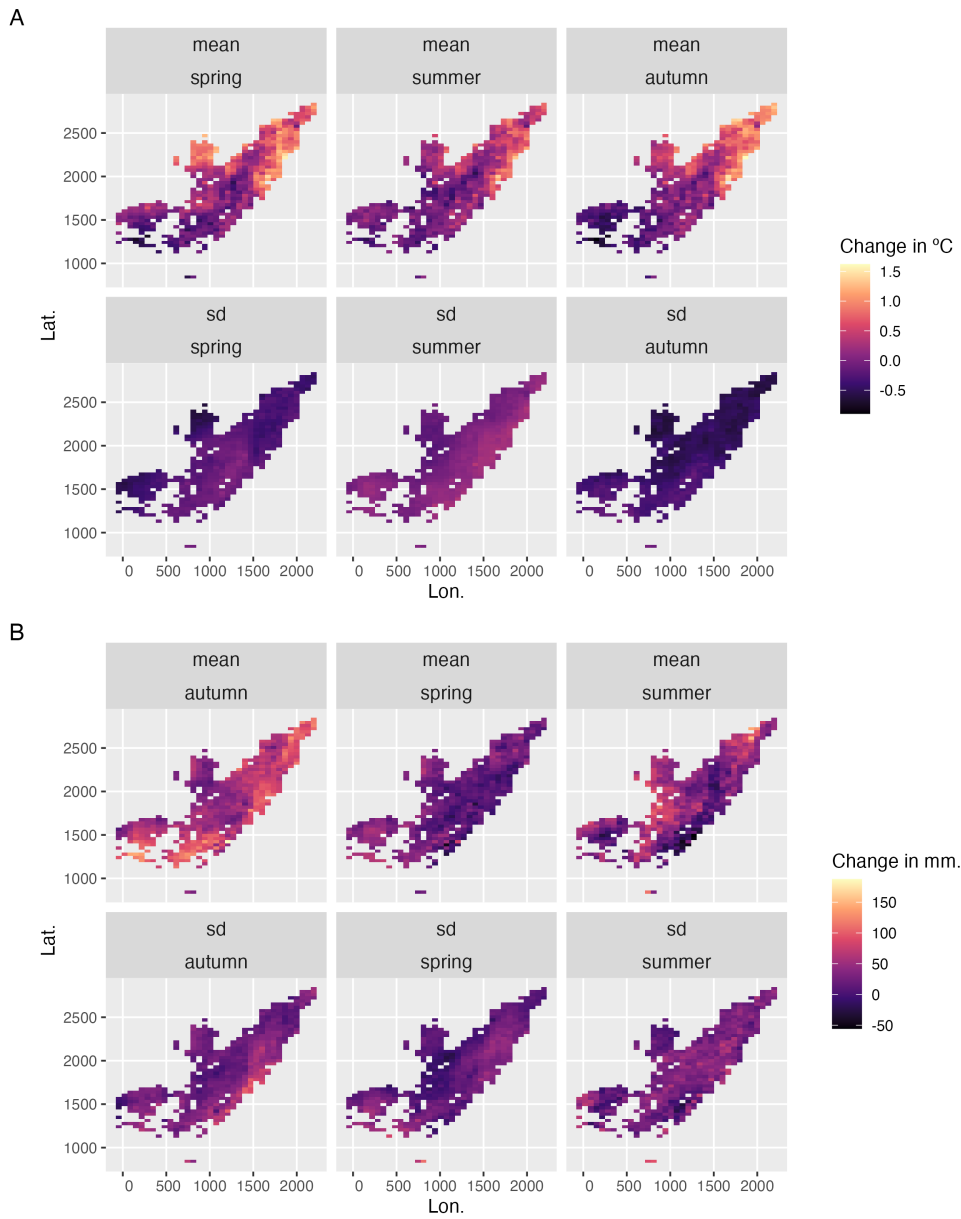


Figure A14: Change in seasonal climate variables between the periods 1895-1925 and 1990-2020 across the distribution of *A. perennans*. Color represents change in (A) seasonal temperature ($^{\circ}\text{C}$) and (B) seasonal precipitation (mm.). Maps show pixels covering the modeled distribution of *A. perennans* used in *post hoc* climate regression analysis.

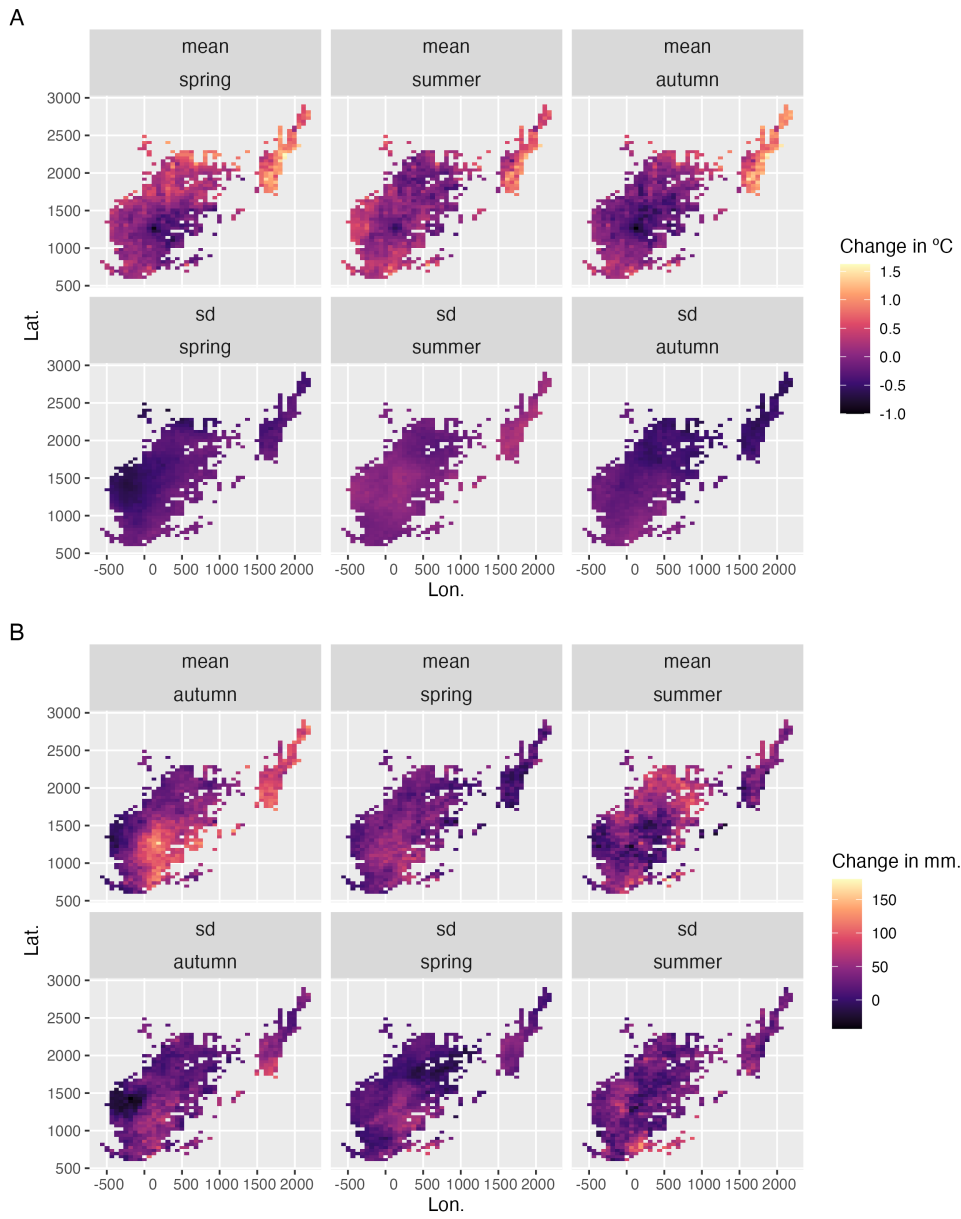


Figure A15: **Change in seasonal climate variables between the periods 1895-1925 and 1990-2020 across the distribution of *E. virginicus*.** Color represents change in (A) seasonal temperature ($^{\circ}\text{C}$) and (B) seasonal precipitation (mm.). Maps show pixels covering the modeled distribution of *E. virginicus* used in *post hoc* climate regression analysis.

Table A1: Summary of herbarium samples across collections (no. of specimens)

| Herbarium Collection | <i>A. hyemalis</i> | <i>A. perennans</i> | <i>E. virginicus</i> |
|---------------------------------------|--------------------|---------------------|----------------------|
| Botanical Research Institute of Texas | 350 | 190 | 198 |
| Louisiana State University | 72 | 38 | 62 |
| Mercer Botanic Garden | 3 | 0 | 6 |
| Missouri Botanic Garden | 210 | 205 | 122 |
| Texas A&M | 100 | 0 | 72 |
| University of Kansas | 134 | 34 | 197 |
| University of Oklahoma | 85 | 34 | 95 |
| University of Texas & Lundell | 183 | 91 | 102 |
| Oklahoma State University | 51 | 10 | 74 |

1035

Supporting Methods

1036

ODMAP Protocol

1037 [Overview](#)

1038 **Model purpose:** Mapping current distribution of *Epichloë* host species.

1039 **Target species:** *Agrostis hyemalis*, *Agrostis perennans*, and *Elymus virginicus*.

1040 **Study area:** Eastern North America

1041 **Spatial extent:** -125.0208, -66.47917, 24.0625, 49.9375 (xmin, xmax, ymin, ymax).

1042 **Spatial resolution:** 0.04166667, 0.04166667 (x, y).

1043 **Temporal extent:** 1990 to 2020.

1044 **Boundary:** Natural.

1045 [Data](#)

1046 **Observation type:** Occurrence records from Global Biodiversity Information Facility and

1047 herbarium collection across eastern North America. We used 713 occurrences records for *Agrostis*
1048 *hyemalis*, 656 occurrence records for *Agrostis perennans* and 2338 for *Elymus virginicus*.

1049 **Response data type:** occurrence record, presence-only.

1050 **Coordinate reference system:** WGS84 coordinate reference system (EPSG:4326 code)

1051 **Climatic data:** raster data extracted from PRISM

1052 [Model](#)

1053 **Model assumption:** We assumed that the target species are at equilibrium with their environment.
1054

1055 **Algorithms:** Maximum entropy (maxent)

1056 **Workflow:** We described the workflow in the method section of the manuscript.

1057 **Software:** All statistics were performed using Maxent 3.3.4 and R4.3.1 with packages terra, usdm,
1058 spThin and dismo.

1059 **Code availability:** Available through this link: <https://github.com/joshuacfowler/EndoHerbarium>

1060 **Data availability:** Data was accessed through open-source R packages *rgbif*. *A. hyemalis*
1061 (GBIF.Org, 2025a), *A. perennans* (GBIF.Org, 2025b), *E. virginicus* (GBIF.Org, 2025c)

1062 [Assessment](#)

1063 We used AUC to test model performance.

1064 [Prediction](#)

1065 We predicted the probability of presence of the host species as a binary maps (presence or absence)

1066 *Mesh and Prior Sensitivity Analysis*

1067 To test the influence that the triangulation mesh and choice of priors has on results, we compared
1068 model results across a range of meshes and priors. We re-ran our model for the mesh used in main
1069 body of the text (Fig. A2), which we refer to as the "standard mesh", and with a mesh with smaller
1070 minimum vertices (finer mesh). Finer scale meshes increase computation time. For each of these
1071 meshes, we ran the model with a range of priors defining the spatial range of our spatial random
1072 effects: 342km (the prior used for presented results), as well as ranges five times smaller (68 km)

¹⁰⁷³ and five times larger (1714 km). We found generally that these choices did not alter the direction
¹⁰⁷⁴ of model predictions, but did influence the associated uncertainty and magnitude of some effects.

¹⁰⁷⁵ For overall temporal trends, we found that models with differing priors predicted consistently
¹⁰⁷⁶ positive relationships over time (Fig. A16).

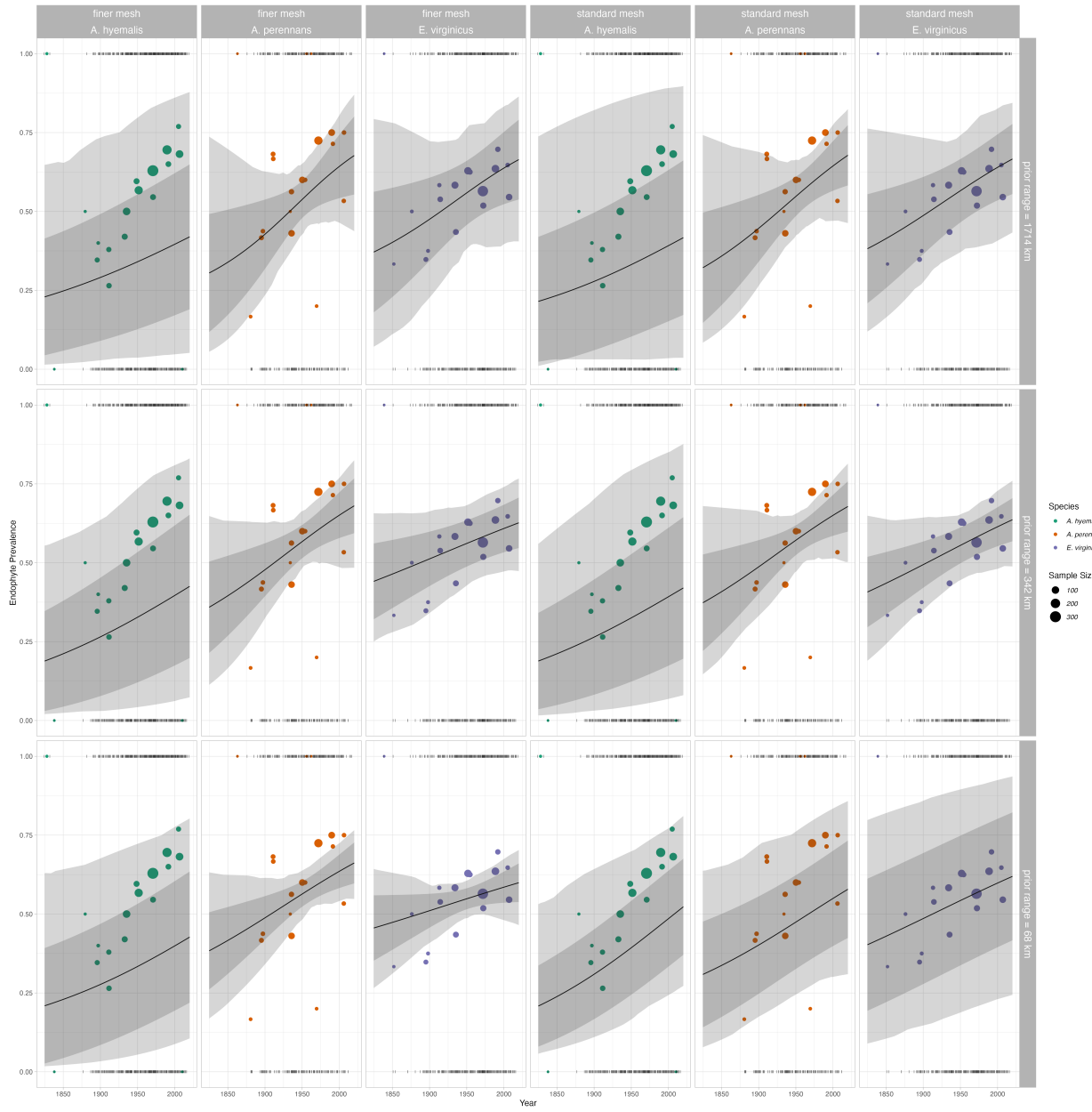


Figure A16: Overall trend in endophyte prevalence evaluated for endophyte prevalence models with different range priors on spatially structured random effects, and for two different triangulation meshes. Data used in model fitting is the same across all panels and as in the main text. Note that these plots, as compared to Fig. 2 in main text, show mean trends and do not incorporate variance associated with collector and scorer random effects.

1077 For spatially-varying temporal trends, we found that models with different priors predicted
1078 consistent spatial patterns in temporal trends, although the range of this prediction varied depending
1079 on the prior and mesh (Fig. A17 - A18). One noteworthy result of this analysis is that combinations
1080 of prior choice and mesh can introduce instability in model fitting. This is evident in A17 panel B
1081 and A18 panel B, where the prior range is smaller than the minimum vertex length of the mesh.
1082 Model fitting takes an extended time period and the model struggles to identify variation across
1083 space. Results with a set of prior ranges (Fig. A17 - A and C; Fig. A18 - A and C) result in
1084 models that estimate trends across space of the same direction and order of magnitude, although
1085 the "smoothness" of these predictions vary.

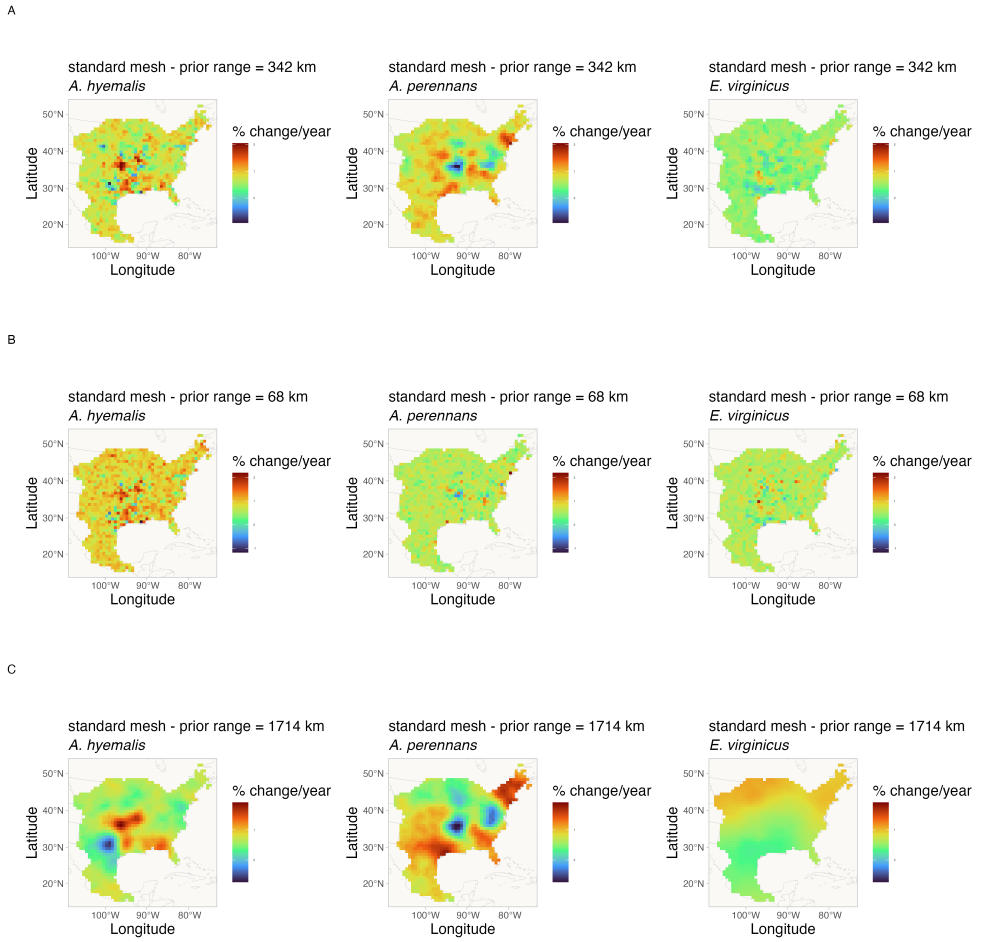
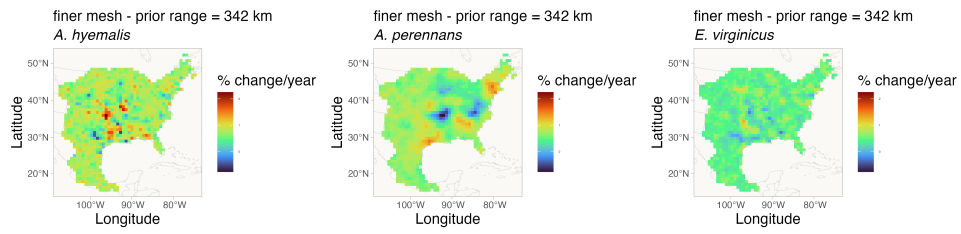
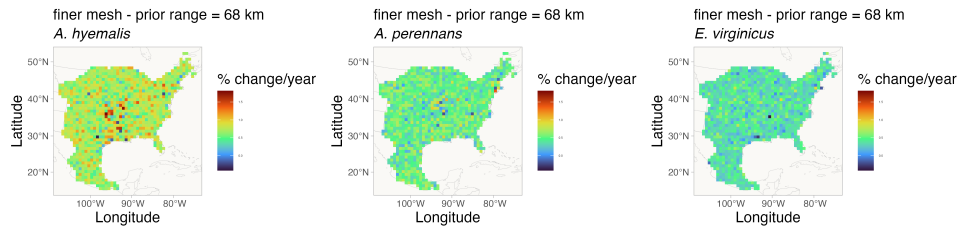


Figure A17: **Spatially-varying trends in endophyte prevalence evaluated for the endophyte prevalence model with different range priors on spatially structured random effects, and for the "standard" mesh.** Data used in model fitting is the same across all panels and as in the main text. Shading indicates the magnitude and direction of predicted trends for each of three host species for each of three prior ranges (rows A-C). Note that each plot has an individual scale bar.

A



B



C

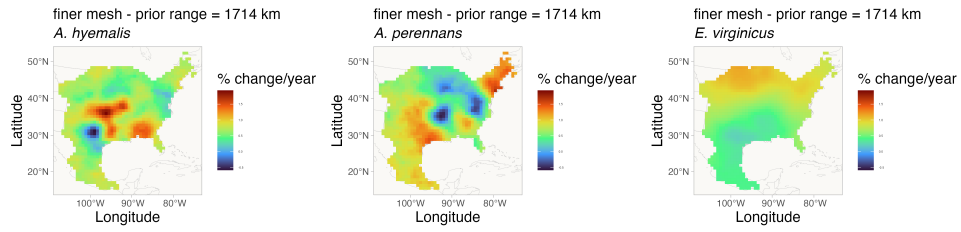


Figure A18: **Spatially-varying trends in endophyte prevalence evaluated for the endophyte prevalence model with different range priors on spatially structured random effects, and for the "finer" mesh.** Data used in model fitting is the same across all panels and as in the main text. Shading indicates the magnitude and direction of predicted trends for each of three host species for each of three prior ranges (rows A-C). Note that each plot has an individual scale bar.

1086

Spatially-biased Sample Size Simulation Analysis

1087 To examine how data that is unevenly distributed across host distributions may influence interpreta-
1088 tion of spatially-varying coefficients, we performed a simulation analysis. Our focal species, *Agrostis*
1089 *hyemalis*, *Agrostis perennans*, and *Elymus virginicus*, are widely distributed grasses across the east-
1090 ern United States that host *Epichloë* fungal endophytes. For logistical reasons, our sampling visits
1091 to herbaria focused on herbaria in the central southern U.S., which resulted in unevenly distributed
1092 data across each host species' range. This is particularly noteable for *Agrostis perennans* which has
1093 the most northern distribution and relatively fewer total collected specimens compared to the other
1094 focal species. Thus, a significant portion in the northeast of this species' range is relatively sparsely
1095 sampled. Our analysis presented in the main text identified this region as having strong increase in
1096 endophyte prevalence. Future visits to herbaria with regional focuses in the Northeastern US would
1097 certainly garner new specimens that could provide valuable insights into shifting host and symbiont
1098 distributions.

1099 *Simulation of spatially-biased symbiont occurrence data*

1100 We simulated datasets with varying levels of missing-ness to examine how this missing-ness influ-
1101 enced the estimation of spatially-varying trend estimates. We first generated 300 data points for
1102 each of three hypothetical species at random positions across an area approximating the scale of
1103 our focal data. Each data point was randomly assigned a year of collection across 200 years. We
1104 then simulated data from a Bernoulli process with trends alternating across nine regions (Fig. A19)
1105 in a 3X3 grid pattern. This grid pattern was intended to create a complex spatial layout of trends,
1106 where trends were either an increase of 1% per year or a decrease of 1% per year.

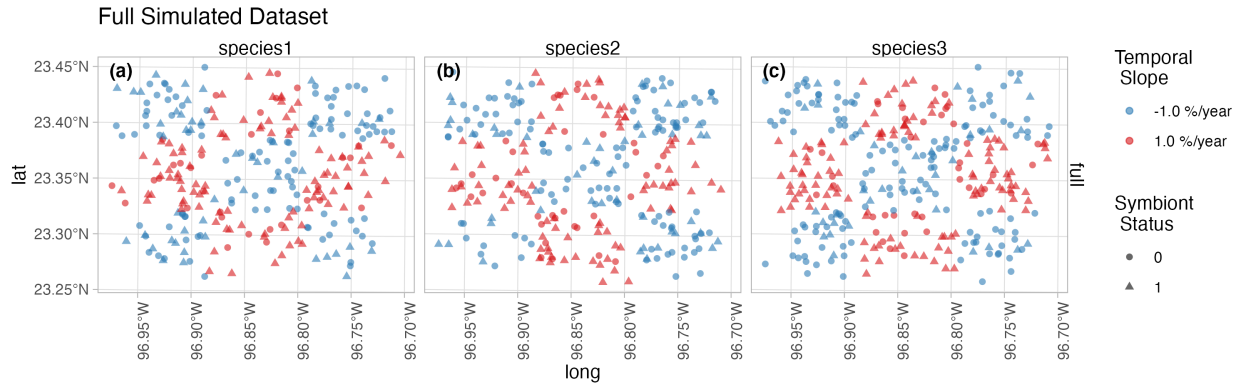


Figure A19: Full simulated dataset of symbiotic association with spatially-varying temporal trends. Color indicates the slope parameter used to simulate trends in endophyte status across nine "regions" for three species. Data are assigned collection years across a period of 200 years. Shape indicates the presence (1) or absence (0) of a symbiont.

From this full data, we generated six additional datasets with missing-ness in the northeast region of the simulated data for hypothetical species 2. The data remained the same for Species 1 and for species 3 across all datasets. For these six datasets, we removed data points at random in six ways: 0% of datapoints in northeast region, 0% of recent datapoints, only 20% of datapoints, only 20% of recent datapoints, only 50% of datapoints, and only 50% of recent datapoints (Fig. A20). We define the datapoints as part of the recent time period if they occur later than the median year. The result is 6 scenarios exploring degrees of spatial and temporal bias.

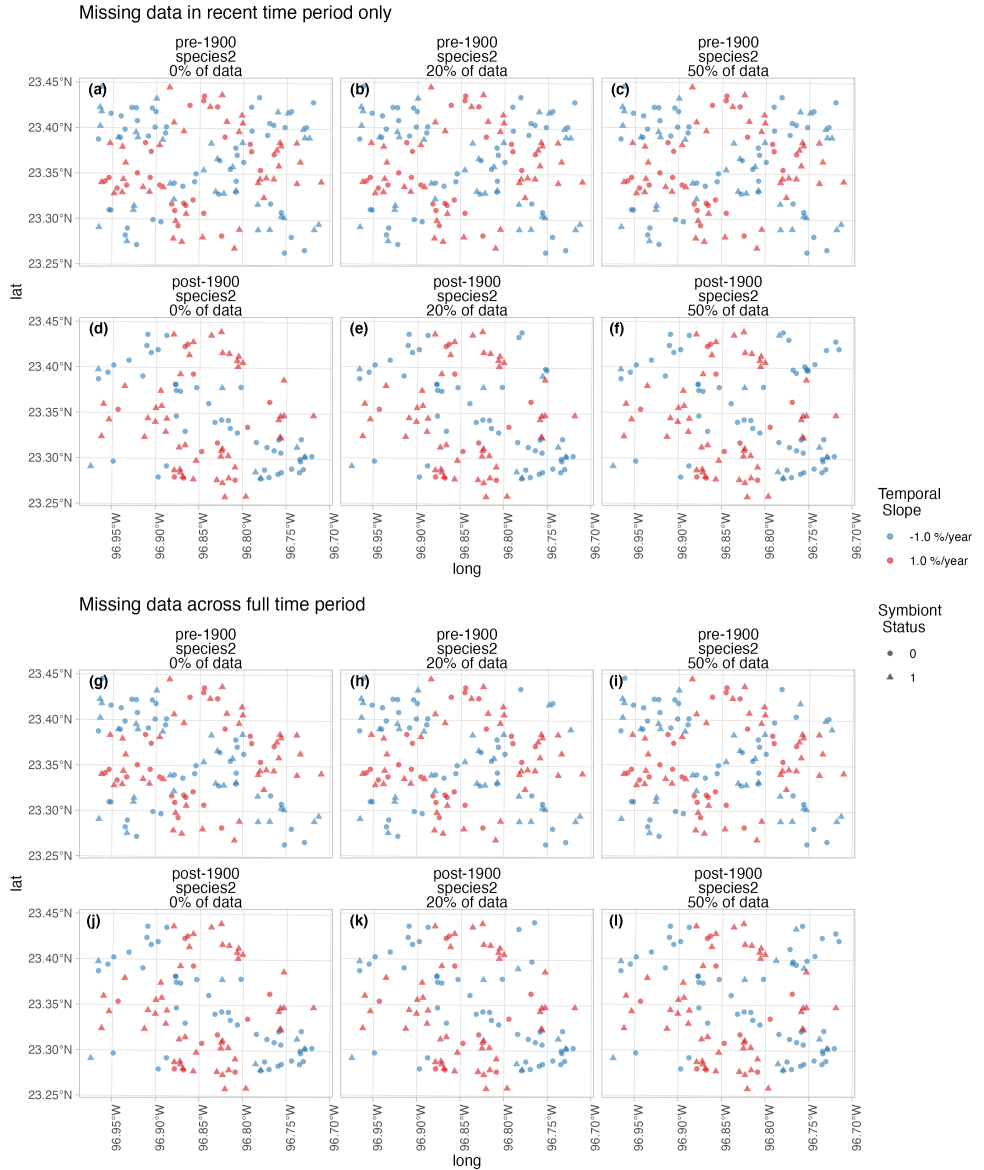


Figure A20: Six simulated datasets representing scenarios of spatially-baised missingness for Species 2. Missingness was imposed in the northeast region for six scenarios: 0% of recent datapoints available (a,d); only 20% of recent datapoints (b,e); only 50% of recent datapoints (c,f); 0% of datapoints across the full time period available (g,j); only 20% of datapoints across the full time period (h,k); and only 50% of datapoints across the full time period(i,l). Missingness was imposed only for hypothetical Species 2; Species 1 and 3 remain as in Figure A19. Color indicates the slope parameter used to simulate trends in endophyte status across 9 regions in a 3x3 grid. Shape indicates the presence (1) or absence (0) of a symbiont.

1114 *Statistical analysis*

1115 We analyzed each dataset with a model given by Eqn. A1 similar in construction to that used in
1116 our central analysis.

$$\text{logit}(\hat{P}_{h,i}) = A_h + T_h * \text{year}_i + \alpha_{h,l_i} + \tau_{h,l_i} * \text{year}_i + \delta_{l_i} \quad (\text{A1})$$

1117 Where symbiont presence/absence of the i^{th} specimen ($P_{h,i}$) was modeled as a Bernoulli re-
1118 sponse variable with expected probability of symbiont occurrence $\hat{P}_{h,i}$ for each host species h . We
1119 modeled $\hat{P}_{h,i}$ as a linear function of intercept A_h and slope T_h defining the global trend in endophyte
1120 prevalence specific to each host species as well as with spatially-varying intercepts α_{h,l_i} and slopes
1121 τ_{h,l_i} associated with location (l_i , the unique latitude-longitude combination of the i th observation).
1122 Similar to the SVC model of our central analysis (Eqn. 1), we estimated a shared variance term
1123 with the spatially-dependent random effect δ_{l_i} , intended to account for residual spatial variation.
1124 However in this analysis we omit i.i.d.-random effects terms associated with collector and scorer
1125 identity (χ_{c_i} and ω_{s_i} in Eqn. 1) for the sake of simplicity.

1126 *Influence of spatially-biased sampling on model interpretation*

1127 Our analysis of the full simulated data shows that our model is suitably flexible to capture complex
1128 spatial patterns in temporal trends (Fig. A21 a-c). Beyond this, the model also qualitatively
1129 captures the spatial patterns in temporal trends even with large amounts of data missingness (i.e
1130 missing up to 80% of the datapoints (Fig. A21 p-r)).

1131 While this analysis is not an exhaustive examination of the influence of sampling bias on our
1132 results for several reasons (including not examining how different strengths in temporal trends,
1133 different spatial arrangements of missing-ness influence model estimates, or different sample sizes
1134 influence results), it demonstrates that the spatially-varying modelling framework implemented in
1135 INLA we employ can suitably recover regional trends even with significant spatially-bias within
1136 data collection, and further the analysis is likely robust to temporally-structured bias (missing data

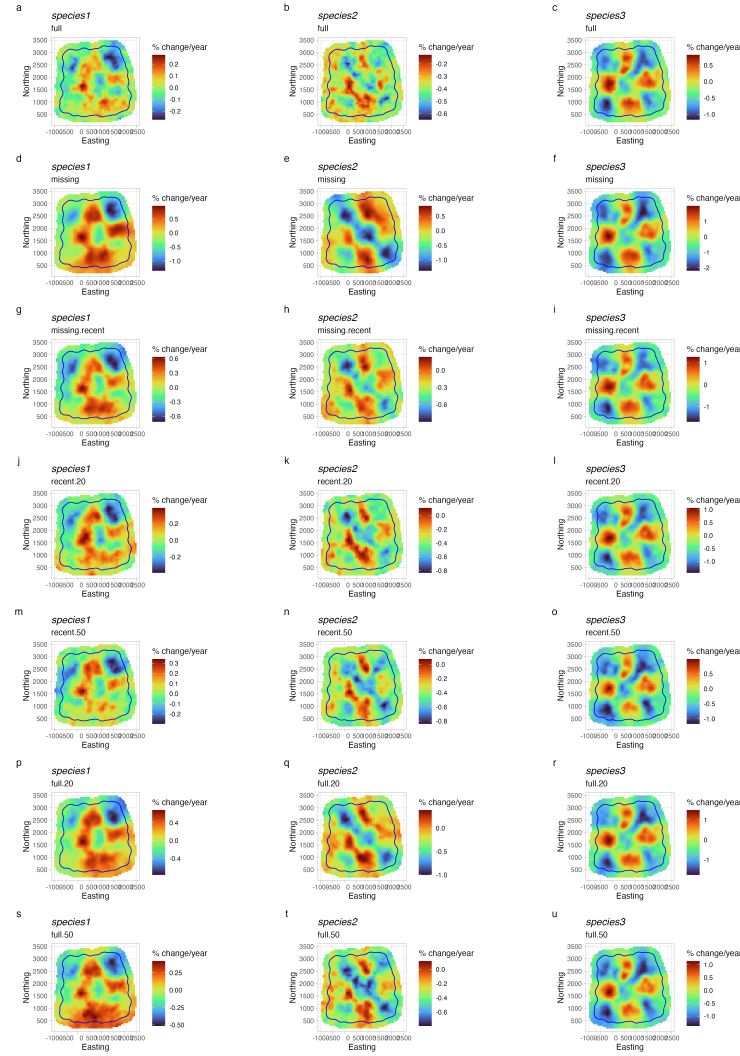


Figure A21: Mean predicted spatially-varying trend in symbiont prevalence across datasets with different levels of missingness. Color indicates the estimated mean temporal trend within each pixel across the simulated data. Panels show estimates for models fit to different levels of missing data for species 2 in the northeast region ((a-c) the full dataset, (d-f) missing all datapoints across entire temporal period, (g-i) missing all datapoints only during the recent period, (j-l) missing 80% of the datapoints only during the recent period, (m-o) missing 50% of the datapoints only during the recent period, (p-r) missing 80% of the datapoints across the entire temporal period, (s-u) missing 50% of the datapoints across the entire temporal period). The mesh boundary that bounds the "full" simulated dataset is plotted in each panel.

1137 within recent collection period). Future work could more fully explore the scenarios that cause
1138 this ability to break down. We expect this simulation reflects what may be a common scenario for
1139 research investigating global change using natural history specimens. Collection effort by trained
1140 taxonomists and professional collectors peaked in the past, and collections contain relatively fewer
1141 modern specimens in many regions. Additionally, most global change research necessarily involves
1142 accessing many specimens across collections. Research efforts such as ours will be unable to access
1143 every specimen from all possible collections. Ongoing digitization efforts will make it possible to
1144 more clearly assess how much data is missing from a particular study compared to the actual
1145 holdings of natural history collections, but ultimately, the decision of what data and collections to
1146 include is a question of sample size and study design.